EFFECT OF THERMO-MECHANICAL TREATMENT ON MICROSTRUCTURE AND TENSILE PROPERTIES OF 38MnSiVS6 MICROALLOYED STEEL

A Thesis Submitted

In Partial Fulfillment of the Requirements

For the Degree of

MASTER OF TECHNOLOGY

by

Shylu John
(Roll No. Y010641)

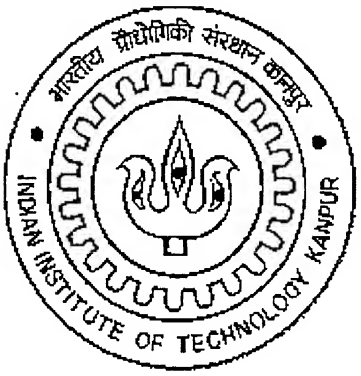

to the

DEPARTMENT OF MATERIALS AND METALLURGICAL ENGINEERING

INDIAN INSTITUTE OF TECHNOLOGY, KANPUR

April, 2002

CERTIFICATE

This is to certify that the thesis entitled "**Effect of thermo-mechanical treatment on microstructure and tensile properties of 38MnSiVS6 microalloyed steel**" by **Shylu John** (**Roll No. Y010641**), has been carried out under my supervision and to the best of my knowledge this work has not been submitted elsewhere for a degree.

Dr. Sandeep Sangal
Professor
Department of Materials and Metallurgical Engineering
Indian Institute of Technology
Kanpur-208016, India

Date: 26/4/02

ACKNOWLEDGMENTS

With a profound sense of gratitude, I express my sincere thanks to my thesis supervisor Dr. Sandeep Sangal for his valuable guidance. I am really grateful for his encouragement throughout the work and for providing me all the facilities and help in every possible way at IIT- Kanpur.

I gratefully acknowledge the help received from Dr. Mungole, Mr. H.C.Srivastava, Mr. Kumar & Mr. B.K. Jain for providing me guidance and letting me benefit from their experience during the experimental work.

I wish to thank Mr. Agnihotri and Mr. Sharma, Metallurgical workshop, for making tensile samples.

I would also like to acknowledge thanks to my freinds Shyam, Subhashish, Sanjiv, Shukla, Vineet, Rao, Himanshu, Harveen, Pinaki, Suhash, Laha, Shankar, S. Sankaran, Prem Singh and Sanjay Chabbra who have helped me throughout the experimental work. I also express my sincere thanks to my friend Satish who has helped me for most of the work in computer related applications and rolling samples.

I must acknowledge the support provided by my beloved parents, brother and sister. I would not have come this far without their unconditional love and support. This thesis is dedicated to them.

Last but not the least, I extend my special thanks to all the staff of Materials and Metallurgical Department and Advanced center for Materials Science, for their unconditional help.

Shylu John

IIT, Kanpur.

ABSTRACT

Microalloyed medium carbon steel 38MnSiVS6 steels have demonstrated superior mechanical properties through thermomechanical treatment. In the present investigation, the effects of processing parameters such as rolling finish temperatures and cooling rate on the microstructure and tensile properties were studied. To yield better mechanical properties, the optimization of the rolling process in the laboratory experiment and rolling mill has been carried out. The microstructure was qualitatively and quantitatively analyzed and correlated to variation in rolling finish temperature and cooling rate. The tensile tests were carried out to obtain correlations of UTS, yield strength and toughness with the above process variables. It has been found that the rolling finish temperature affects the microstructure and tensile properties, but cooling rate plays much greater influence. The tensile properties of thermo-mechanically treated samples were correlated with changes in microstructure, i.e. volume fraction and aspect ratio of ferrite, matrix phase and initial grain size. The microstructural changes due to deformation start temperature were also studied by giving another thermomechanical treatment. Finally, deformation start temperature above 1150°C and water quenching sequence of 38MnSiVS6 steel plates have been suggested after hot rolling of plates.

TABLE OF CONTENTS

LIST OF FIGURES

Figure

LIST OF TABLES

Table

CHAPTER 1

INTRODUCTION AND OBJECTIVES

Improved quality has moved segments of the industry farther away from commodity-grade markets. Consumers are demanding higher-quality products, and steel companies have responded accordingly with new products such as lighter, stronger, more formable automotive sheet and other products to satisfy niche markets. However, the technological improvements in steel properties are potentially a double-edged sword. While these advances allow steel companies to find new markets or prevent the substitution of alternate materials in existing markets, the end result may well be lower consumption of steel. For instance, the development of high-strength low-alloy (HSLA) steels in sheet and forged applications has reduced demand in this area because HSLA steel is 200–400 percent stronger than regular carbon steel. A 50-percent increase in strength reduces weight by 30 percent while still providing equivalent properties with respect to dent resistance, formability, etc. Microalloyed forging steels have been developed to improve the competitiveness of wrought steel components, especially in the automotive sector, achieving the desired properties in as forged condition [1].

Quenching and tempering (QT) has been the conventional route for obtaining the desired mechanical properties in steel after forging. Due to various technical and economical shortcomings associated with QT treatment, continuous cooling (CC) from forging temperature was its alternative [2]. In this treatment changes in the microstructure are accomplished through controlled variation in the cooling rate. By control of the cooling rate, fineness of pearlite can be controlled and hardness values comparable to that obtained by QT treatment can be achieved [3]. The deformation temperature is also very important parameter. Decrease in the deformation temperature has been long been known to bring about an increase in the strength value. It is also certain that lowering the deformation temperature will increase the ferrite fraction formed, aided by the increase in the nucleation sites in the unrecrystallized austenite. These two opposing observation

have raised strength levels along with an increase in amount of softer ferrite, incase forging as mode of deformation [3].

In two-step cooling (TSC) process, two different cooling rates are involved after the forging treatment as shown in Fig. 1.1. The first slow step (with cooling rate T_1) leads to formation of ferrite. The deformation induced ferrite forms at comparatively high, consequently ferrite is polygonal and has higher carbon in it. This gives better toughness and also higher strength because of high carbon content. Moreover at high temperature the supersaturated carbon in ferrite diffuses and stabilizes the adjacent austenite. This suppresses pearlite transformation and as a consequence aids the bainitic formation. Second cooling step (cooling rate T_2), of accelerated kind, lead to the formation of harder phase such as bainite and martensite [4]. The volume fraction of both soft and hard, phase in the microstructure is function of forging temperature (To) and quenching temperature (T_Q) [5].

The following objectives were identified for forge grade microalloyed steels with rolling as a mode of deformation:

1. To study the effect of deformation start temperature on microstructure.
2. To establish the rolling finish temperature and subsequent cooling treatment to be given on forge grade microalloyed steel plates.
3. To characterize the microstructures (using qualitative and quantitative analysis) obtained after thermomechanical treatment.
4. To correlate the microstructural parameters with the tensile properties obtained after processing.

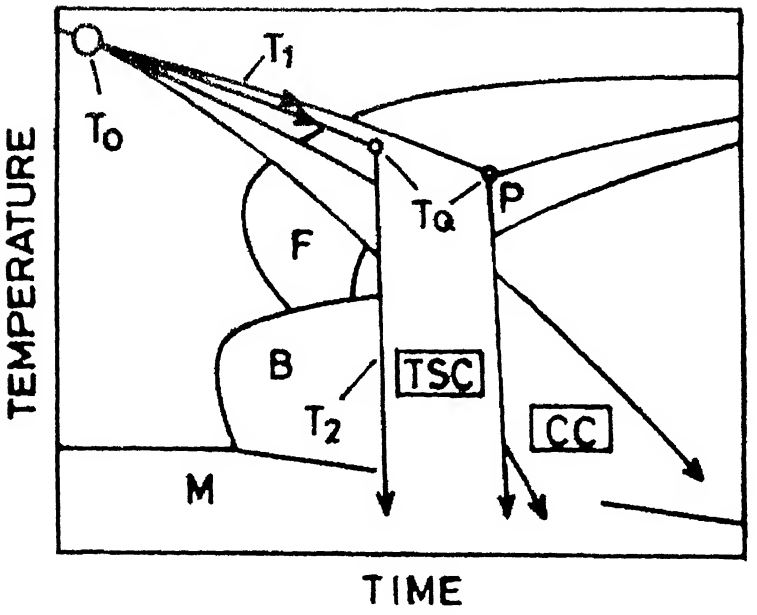

Fig.1.1: Processing schedules for two-step cooling

CHAPTER 2

LITERATURE REVIEW

2.1 The rationale of microalloyed high strength steels

The motivation for the use of high strength low alloy (HSLA) steels is cost reduction. Higher strength steels can sustain service loads over thinner sections, thus providing weight savings and use of less steel. Lower costs can also be realized if microalloyed steels can replace alloy steels containing significant amounts of expensive elements like Nickel, Chromium or Molybdenum. However, the most significant cost reduction provided by microalloyed HSLA steels is the elimination of expensive heat treatment and their use in the mill processed condition, as rolled, which provides considerable energy saving. As-rolled microalloyed HSLA steels exhibit properties, which are comparable in many ways to those of normalized or quenched and tempered products, yet avoid the cost of heat treatment, handling, energy decarburization, scale loss (oxidation) etc.

In terms of mechanical properties, the heat-treated (quenched and tempered) low alloy steels offer the best combination of strength and toughness (Table 2.1) [6]. However, these steels are available primarily as bar and plate products and only occasionally as sheet and structural shapes. In particular, structural shapes (I-beams, channels, wide flanged beams, or special sections) can be difficult to produce in the quenched and tempered condition because shape warpage can occur during quenching. Heat-treating steel is also a more involved process than the production of as-rolled steels, which is one reason why as-rolled steels are an attractive alternative. The as-rolled HSLA steels are also commonly available in all the standard wrought forms (sheet, strip, bar, plate and structural shapes).

In general the rationale behind the development of these steels can be summarized as:

Table 2.1 General comparison of mild steel with various high strength steels[Metals Handbook, 1990]

Steel	Chemical Composition(%)[a] C (max.)	Mn (max.)	Si (min.)	Other	Min. Yield Strength(Mpa)	Min.UTS (Mpa)	Min.Ductility[b] (%)
Low-Carbon steel	0.29	0.60	0.15	(c)	170-250	310-445	23-30
As-hot rolled C-Mn steel	0.40	1.00	0.15	.....	250-400	415-690	15-30
HSLA steel	0.08	1.30	0.15	0.02 Nb	275-450	415-550	18-24
Heat treated C steel Normalized[c]	0.36	0.90	0.15		200	415	24
Quenched and Tempered	0.20	1.50	0.15	5 ppm B	550-690	660-760	18
Q and T low-alloy steel	0.21	0.45	0.20	0.45 Mo, 50 ppm B	620-690	720-800	17-18

[a] Typical compositions include 0.04% P (max.) and 0.05% S (max.)
[b] Elongation in 50 mm gage, [c] If copper is specified, the minimum is 0.20%.

- Filling the yield strength gap between the simple carbon and mild steels with σ_y ~300Mpa and heat-treated low alloy steels with σ_y ~850Mpa with mill processed microalloyed steel not requiring a separate heat treatment operation.
- Producing high yield strength so that a greater load bearing capacity is possible with thinner sections.
- Decreased processing costs, and obtaining a higher yield strength material, by using mill-processed steel with consequent energy conservation.
- A minimal use of expensive and scarce alloying addition, with the consequent conservation of strategic scarce materials.
- High weldability.
- A high resistance to brittle cleavage and low energy ductile fracture, and a low ductile-brittle transition temperature.
- Ability to cold form to some extent, particularly by bending and good ductility and toughness through the thickness of rolled strips and plates.
- Optimal property combinations per unit cost.

Three main classes of material microstructures have met these requirements:

Steels comprising ferrite – pearlite microstructures, will be the main subjects of this discussion. Acicular ferrite structures, which may be considered to be very low carbon variants of bainitic steels developed in the early 1950's. These are less popular than the ferrite-pearlite structures, largely due to increased cost. Dual phases microstructures, which were developed specially to increase the formability and aimed particularly for use in the manufacture of automobile components.

2.2 Classification

HSLA steels can be divided into the following six categories:

- Weathering steels, which contain small amounts of copper and phosphorous, and display improved atmospheric corrosion resistance and solid solution strengthening.
- Microalloyed ferrite-pearlite steels, which contain very small addition of strong carbide or carbonitride forming elements such as niobium, vanadium and/or titanium for precipitation strengthening, grain refinement and transformation control.
- As-rolled pearlitic steels, which may include carbon-manganese steel but which also have small addition of other alloying addition to enhance strength, toughness, formability and weldability.
- Acicular ferrite steels, which are low carbon steels with an excellent combination of high yield strength, formability, weldability and toughness.
- Dual-phase steels, which have a microstructure of martensite dispersed in a ferrite matrix and provide a good combination of ductility and high tensile strength.
- Inclusion shape controlled steels, which provide improved ductility and toughness by small addition of calcium, zirconium or titanium, or rare-earth elements so that the shop of sulfide inclusions are changed from elongated stringers to small, dispersed, almost spherical globules.

2.2.1 Microalloyed Ferrite-Pearlite Steels

The yield strength σ_y is given in general terms by:

$$\sigma_y = \sigma_i + \sigma_s + \sigma_p + \sigma_d + k_y d^{-1/2}$$

where σ_i is the friction stress opposing dislocation motion, σ_s is the contribution from solid solution strengthening, σ_p is due to precipitation strengthening, σ_d is because of dislocation strengthening, k_y is the dislocation locking term and d is the ferrite grain diameter. Using well known theories of strengthening and work hardening of structures comprising unreformed particles in an unreformed matrix [7,8] it has been shown that the flow stress and the work hardening rate can be predicted accurately [9,10]. The flow

stress and the work hardening rate are controlled by volume fraction and the particle size of the M-A constituent. Theories predict that both the flow stress and the work hardening rate should be related linearly to the reciprocal of the square root of the size of the M-A particles.

These steels use additions of niobium and vanadium to increase the strength of hot rolled steel without an increase in the carbon and/or manganese contents. the various types of microalloyed ferrite-pearlite steels include :

- Vanadium-microalloyed steels
- Niobium-microalloyed steels
- Niobium-molybdenum steels
- Vanadium-niobium microalloyed steels
- Vanadium-nitrogen microalloyed steels
- Titanium-microalloyed steels
- Niobium-titanium microalloyed steels
- Vanadium-titanium microalloyed steels

Vanadium containing steels are used in the hot rolled condition and also in the controlled-rolled, normalized, or quenched and tempered condition. Strengthening from vanadium averages between 5 and 15 MPa per 0.01 wt.% V [11] depending on carbon content and cooling rate. An optimal level of precipitation strengthening occurs at a cooling rate of about $170^{\circ}Cmin^{-1}$. Manganese content and ferrite grain size also effect the strengthening of vanadium microalloyed steels [12]. The effect of manganese on precipitation strengthening is more in vanadium steels than in niobium steels.

2.3 Role of microalloying elements

Alloying elements are selected to influence the transformation temperatures so that the transformation of austenite to ferrite and pearlite occurs at a lower temperature during air-cooling. This lowering of the transformation temperature produces a finer grain transformation product, which is the main source of strengthening. At the low carbon levels typical of HSLA steels, elements such as silicon, copper, nickel and phosphorous are particularly effective for producing fine pearlite.

The microalloying elements Nb, V and Ti are added singly or in combination to what are essentially carbon-manganese steels, to produce the HSLA steels. These three microalloying elements have very different effects due to their different affinities for carbon and nitrogen. Microalloying elements are added to steel for two main purposes, namely, to grain refine and/or precipitation strengthening. Both effects result from the precipitation of microalloy carbides, nitrides or carbonitrides. These precipitates in ferrite can prevent ferrite grain growth during or after the transformation and so have an indirect grain refining effect. It must be emphasized, however, that microalloy carbides/ nitrides precipitated in the austenite do not cause strengthening

2.3.1 Solubility Effects

The solubility of the microalloy carbides/nitrides in austenite decreases in the following order: TiN, NbN, TiC, VN, NbC, VC and the same order is followed for the solubility in ferrite in which the solubility is some two orders of magnitude smaller than in austenite. A general solubility product equation is:

$$\text{Log } [M][X] = A/T + B$$

Where [M] and [X] are the weight percent of microalloying element and C or N dissolved in the austenite at T Kelvin, and A and B are constants.

2.3.2 Grain Refinement

The essence of grain refinement is to prevent grain boundary migration and grain growth. This may be done either by grain boundary solute segregation introducing a frictional drag on the moving boundary or by grain boundary pinning particles which decrease the grain boundary area and hence the overall grain boundary energy.

If the grain size is to remain small at the high temperature in the austenite region, such as what is used for reheating for hot rolling, especially for recrystallization controlled rolling (RCR), two conditions are to be satisfied [13]:

(i) the volume fraction of pinning particles must remain large, and

(ii) the pinning particles must grow very slow at the temperature involved.

The low solubility and general thermodynamic stability causes TiN to be the most resistant of the microalloying carbides/nitrides to particle coarsening, and thus the most effective grain boundary pinning phase. This partially explains why Ti microalloying is used in recrystallization controlled rolled steels.

2.3.3 Precipitation Strengthening

In Nb steels the strengthening precipitates are predominantly NbC and in Ti steels TiC. Due to the restricted solubility of Ti in the austenite, strengthening by TiC requires rather high Ti additions compared to the 0.01/0.02 wt% required for optimal grain refinement. A higher austenizing temperature will also be required. Thus, Ti additions are not predominantly used for precipitation strengthening in many steels. In contrast, due to the increased solubility of VC, V additions are mainly made for precipitation strengthening and unlike NbC, the solubility and hence the precipitation potential is not greatly limited by the carbon, eight due to additional VN precipitation or N being dissolved in VC as V(CN). Also, decreasing the transformation temperature produces finer precipitates, and greater precipitation strengthening.

2.3.4 Alloying Elements

Vanadium: Precipitation strengthening is one of the primary contributors to strength in microalloyed steels; it is most readily achieved with vanadium additions in the 0.03 to 0.10-wt% range. Vanadium also increases toughness by stabilizing dissolved nitrogen. The impact transition temperature also increases when vanadium is added.

Niobium: Niobium can also have a strong precipitation strengthening effect provided it is taken into solution during reheat and is kept in solution during forging. Its main contributions, however, are to form precipitates above the transformation temperature and to retard the recrystallization of austenite, thus promoting a fine- grained microstructure having improved strength and toughness. Concentrations vary from 0.02 to o.1o% Nb.

Titanium: Titanium can behave both as a grain refiner and precipitation strengthener, depending on its content. At composition greater than 0.05 wt% titanium carbides begin to exert a strengthening effect. However, at this time, titanium is use commercially to retard austenite grain growth and thus improve toughness. Typically titanium concentrations range from 0.01 to 0.02 wt.%.

Molybdenum: Molybdenum in hot rolled HSLA steels is used primarily to improve hardenability when a transformation product other than ferrite or pearlite is desired. It also greatly simplifies the process controls necessary in the forge shop.

Manganese: Manganese is generally present in larger quantity in HSLA steels than in structural carbon steels. It functions mainly as a mild solid solution strengthener in ferrite and also provides a lowering of the austenite to ferrite transformation temperature. In addition, it improves the notch toughness of HSLA steels. In steels for welding application Mn should be kept below some maximum value that depends on the overall composition but mainly on the carbon content.

Silicon: Silicon is usually present in fully deoxidized steels in amounts up to 0.35%. Silicon has a strengthening effect in low alloy structural steels. In larger amounts it reduces scaling at elevated temperature. Silicon has a significant effect on yield

strength enhancement by solid solution strengthening. Effects of selected elements on the various factors discussed above are given in Table 2.2.

Table 2.2 Effect of selected elements on the properties of microalloyed steels [14]

Elements	**Precipitation strengthening**	**Ferrite grain refinement**	**Nitrogen fixing**	**Structure modification**
Vanadium	Strong	Weak	Strong	Moderate
Niobium	Moderate	Strong	Weak	None
Molybdenum	Weak	None	None	Strong
Titanium	Strong (<0.05%Ti)	Strong	Strong	None

2.3.5 Making nitrogen a friend, not a foe

Two new developments in steel making and steel processing – the growth of the electric-arc furnace (EAF) and processing by thin-slab casting – have contributed to further cost reduction in the production of microalloyed steels. EAF steel making is growing rapidly worldwide because it is less capital-intensive than the conventional processes used by integrated-steel producers. Virtually all-new steel making capacity, added either by mini-mills or integrated producers, uses electric arc furnaces. Soon, 50% of the worlds steel making or about 400 million tons annually will be made in these facilities.

In a scrap-based EAF practice, the nitrogen content is 70-100 ppm or 2 to 3 times higher than that typical of the basic-oxygen or BOF practice. Modifying the slag practice or changing the feedstock can reduce the nitrogen level of steels made in an EAF. Both these methods can increase costs. Free nitrogen, in solution in ferrite, has serious detrimental effects, such as aging and brittleness. During concasting, excessive nitrogen may increase possible transverse or longitudinal cracking. Fears are also frequently

expressed about the detrimental effects of nitrogen on weldability. However, the harmful effects of nitrogen may be neutralized by nitrogen-binding elements which, acting as scavengers, remove nitrogen from solid solution in ferrite. Aluminum and titanium are effective scavengers; however, niobium (columbium) is not an effective nitrogen-binding element in high-strength, low-alloy steels. In niobium steels, niobium carbonitrides are only present when the carbon-to-nitrogen ratio ranges between 1:1 and 4:1. Thus, the effect of niobium depends on the nitrogen content of the steel.

Among the various microalloying elements, vanadium has a unique dual effect on nitrogen. Vanadium not only neutralizes nitrogen by forming VN compounds but also uses nitrogen to optimize the precipitation reaction. Enhanced nitrogen increases the supersaturation in ferrite and promotes a more active nucleation of V(C, N) particles, as shown in Fig.2.1 [15]. Consequently, the interparticle distance is reduced (Fig.2.2.) and the strengthening effect of precipitation is increased. In the presence of nitrogen, less vanadium is needed to achieve the desired yield strength. As a result, vanadium effectively converts nitrogen, previously considered an impurity, into a valuable alloy that helps strengthen steel [16].

The pioneering efforts of the Nucor Steel Corporation in commercializing thin-slab casting have dramatically changed the economics of hot-band production. The revolutionary effect of this new process can be compared to two previous developments which have changed the economics of steel production: the switch of steel making from open hearths to a basic-oxygen (BOF) converter and the replacement of ingot casting by continuous casting [17].

The thin-slab-casting process converts in-line liquid steel into a marketable product. The process incorporates a series of steps that contribute to either cost reductions or to property improvements. The rapid solidification in the mold accounts for the small size of globular inclusions, which do not elongate during hot rolling. This promotes isotropic properties, such as bendability, in longitudinal or transverse directions. Near net-shape dimensions of the slab (50-70 mm) facilitate rolling to an aim thickness of 1 mm (or less), allowing hot-rolled steel to economically replace cold-rolled sheet. In-line processing permits the slab to be directly charged into the rolling mill, contributing to

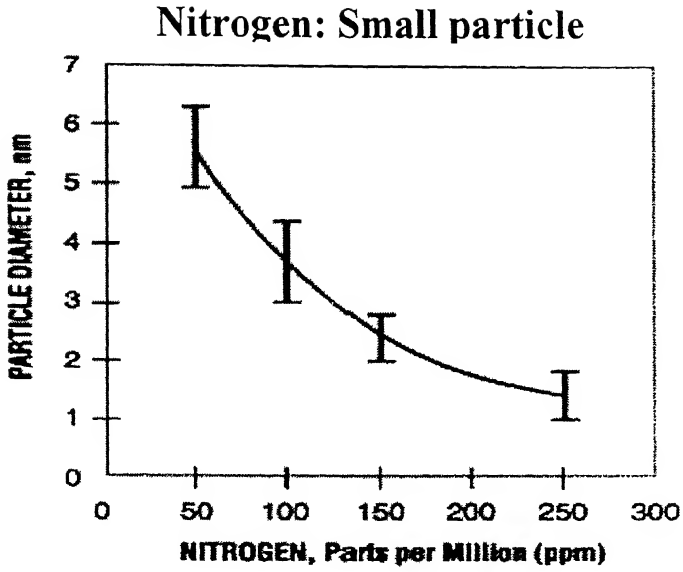

Fig. 2.1: Increasing the nitrogen content promotes nucleation, forming smaller vanadium-nitride particles.

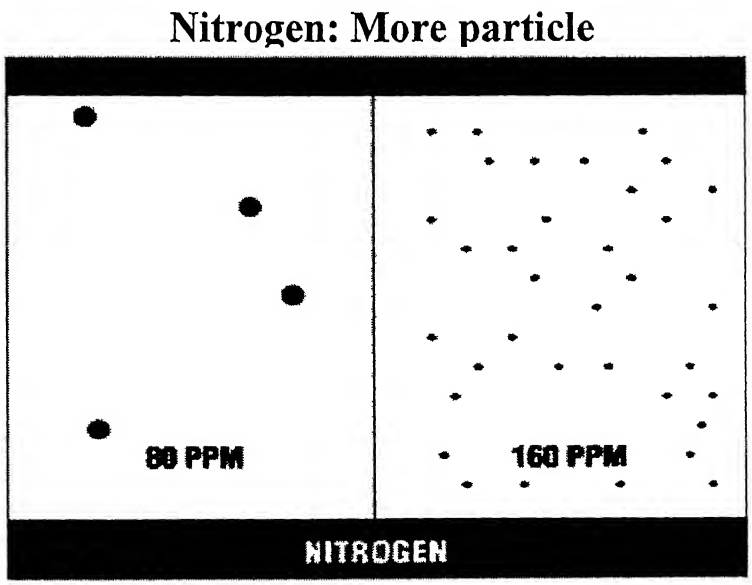

Fig. 2.2: Reducing the particle diameter of precipitates from 4 to 2nm gives eight times the number of precipitates in a given volume of steel. The larger number of small precipitates gives more efficient strengthening by reducing interparticle spacing.

energy savings. The amount of deformation per pass is 2 to 3 times higher than that on a hot-strip mill rolling thick slabs. Excellent microstructure and properties are obtained in a 15-mm-thick strip for a total deformation of less than 4:1 [18].

Because of lower hot-rolling costs, the market share for hot bands produced by thin-slab casting is being increased at the expense of high-cost integrated producers. In developing the concept of replacing carbon steels with microalloyed steels, we will limit our choice initially to strip made by thin-slab-casting technology.

2.4 Applications of HSLA steels

HSLA steels were used as structural shapes and plates in the early 1960's because of their ability to weld with ease. By the early 1970's, they were also used in pipelines at both elevated temperature and severe arctic conditions. Later in 1970's, concurrent with the energy crisis, another dominant application involves the use of HSLA steels to reduce the weight of parts and assemblies in trucks and automobiles. In the 1980's, bars, forgings and castings have emerged as applications of particular interest. Shapes such as elbows and fittings for pipelines are also being cast out of microalloyed steel. HSLA steels are used in a wide variety of applications, and their properties can be tailored to specific applications by a sustainable combination of composition and microstructures obtained by processing in a mill. For example, low carbon and closely controlled carbon equivalent values provide good toughness and weldability. Good yield strength and fracture toughness results from a fine grain size.

Oil and gas pipelines. While tensile strength is a key requirement in pipelines, other properties are no less critical for the fabrication and operation of oil and gas pipelines. They include weldability, fracture toughness and corrosion resistance, which are met by HSLA steels.

Automotive Applications. Experience in the application of cold and hot rolled HSLA sheet in automotive applications indicates the importance of requirements with respect to stiffness, crash behaviors, fatigue life, corrosion resistance, acoustic properties and of- course, formability and weldability. In addition to improvement in mileage per

unit fuel consumption through weight reduction, benefits may be found in increasing payloads without a change in fuel consumption. Candidate applications here include trucks, rail cars, off-highway vehicles and ships. Ship applications are however limited by buckling and stiffness considerations.

Offshore applications. The essential characteristics of steels for these applications include:

- Yield strength in the regions of 350 to 415 MPa.
- Good weldability.
- High resistance to lamellar tearing.
- Lean compositions to minimize preheat requirements.
- High toughness in the weld heat-affected zone.
- Good fracture toughness at the designated operating temperatures.

Some of these goals have been realized through a reduction in impurities such as sulphur, nitrogen and phosphorus in the steel making process. Controlled rolling and accelerated cooling of niobium steels have allowed a reduction in carbon contents, which is important to enhance weldability. Modification of sulphide inclusions is done by additions of rare-earth elements or calcium to form spheroidal inclusions. This approach usually results in both the elimination of lamellar tearing and an improvement in transverse impact properties. Bars, forgings and castings have emerged as the latest area of opportunity for microalloyed HSLA steels, and there has been a rapid assimilation of technologies developed in other product areas. In particular, the search is on higher strengths, elimination or reduction of heat treatments, simplified cold finishing or machining operations, and improved toughness, machinability and weldability.

2.5 Thermo-mechanical treatments for sheets, strips and plates

The aim of processing of HSLA steel is to condition the austenite that it transforms to produce the finest ferrite grain size in order to achieve the greatest yield strength consistent with optimal toughness and ductility.

2.5.1 Thermomechanical working and controlled rolling

It is required that in order to produce the finest ferrite grain size, the thermomechanically worked austenite should recrystallize during transformation, exhibit a high ferrite nucleation rate and a low ferrite growth rate. In addition, the nucleation and growth of microalloy carbides/nitrides are of utmost importance.

The requirement to produce the necessary fine ferrite grain size is greatest area of austenite grain boundary for ferrite nucleation. Such nucleation can occur on deformation bands in the uncrystallized austenite, on the recovered sub-structure boundaries, particularly if these contain precipitates, and on undissolved carbides/nitride particles [19].

In order to obtain the finest possible ferrite grain size, not only the initial austenite grain size should be as fine as possible but also the temperature of rolling should be as low as possible provided it is above the recrystallization stop temperature, and the rolling strain should be as large as possible.

Current steels tend to employ combinations, e.g. Nb-V. The NbC or VN (using enhanced nitrogen) tend to restrict grain growth, whilst the more soluble VC is used to precipitation strengthen the ferrite. Microalloying additions also have another important effect during controlled rolling, in that they retard recrystallization. The effect seems to be in the ascending order of effectiveness: Mn, Al, V, Nb an Ti on n atomic percentage basis is well established that the recrystallization stop temperature of the austenite increases in the increasing order: V, Al, Ti, Nb. The importance of retardation on recrystallization during controlled rolling lies in the ability to use a low finish rolling temperature to produce elongated uncrystallized austenite grains, which can transform to very fine polygonal ferrite [20].

2.5.2 Conventional low temperature controlled rolling

Tanaka (1981) identified the processing parameters to condition the austenite to produce the finest ferrite grain size and optimum precipitation strengthening, using conventional low temperature controlled rolling as [21]:

(a) a low reheating temperature to produce a fine initial austenite grain size;

(b) austenite grain refinement;

(c) suitable pass schedules and reductions to obtain in the initial roughing passes a fine, uniform recrystallized austenite;

(d) delay between roughing in the recrystallization regime and finishing in the unrecrystallized regime;

(e) suitable reductions in the unrecrystallized regime below the recrystallization stop temperature, and in some cases finishing below the Ar3;

2.5.3 Recrystallization Controlled Rolling

Much work has been done in recent years on recrystallization controlled rolling [22,23,24,25]. An initial very fine austenite grain size is required prior to rolling and this is achieved by addition of Ti to form TiN. Such particles very effectively pin the austenite grain boundaries and inhibit grain growth. Rolling is then carried out above the recrystallization stop temperature so that repeated recrystallization occurs during deformation sequences. Heavy rolling reductions at the lowest possible temperature above the recrystallization stop temperature produces the finest recrystallized austenite grain size. The fine recrystallization austenite grains have a high grain boundary surface area per unit volume, i.e. a high S_v, and thus provide many ferrite nucleation sites. Hence, on transforming the austenite, a very fine ferrite grain size is obtained which can be 10μm or less and is produced from a recrystallized austenite 20μm or less [26,27]. Using a 0.09 wt% C, 1.4 wt% Mn, 0.01 wt% Ti, 0.08 wt% V, 0.013 wt% N steel, recrystallization controlled rolled and cooled at 9°C/s, one can obtain a yield stress of 450/500 MPa with as ITT of 70oC [26] which is comparable with the properties produced by conventional low temperature controlled rolling.

2.5.4 Controlled cooling

The purpose of controlled or accelerated cooling is to produce the optimal γ to α transformation temperature, so that the finest ferrite grain size is achieved, together with optimal strengthening by microalloy carbide/nitride precipitation. A useful method of refining the ferrite grain size for a given austenite grain size will decrease the transformation temperature. This increases the ferrite nucleation rate and the effect may be achieved by alloying or by decreasing the cooling rate. The greater the cooling rate or lower the coiling temperature, the finer is the ferrite grain size from the given austenite structure.

Using the well-known solubility limit to assess the volume fraction precipitates, and the observed effects of coiling temperature on both the ferrite grain size and the precipitate size, it is possible by employing a Hall-petch equation and an Ashby. Orowan precipitation strengthening equation, to calculate the yield stress as a function of coiling temperature. This can be converted into a monogram for process control.

2.6 Morphology of ferrite in medium carbon microalloyed steel

Ferrite which grows by a diffusional mechanism can be classified into two main forms: allotriomorphic ferrite and idiomorphic ferrite. The term " allotriomorphic" means that the phase is crystalline in internal structure but does not show its appearance in microstructural form. Infect, allotriomorphic ferrite, which nucleates at the prior austenite grain boundaries, tends to grow along the austenite boundaries at the rate faster than in the direction normal to the boundary plane, so its shape is strongly influenced by the presence of the boundary and hence does not necessarily reflect the symmetry of its internal structure. The term idiomorphic implies that the phase concerned has faces resembling its crystalline structure; in steels, idiomorphic ferrite is taken to be that which has roughly equiaxed morphology. Idiomorphic ferrite usually forms intragranularty at inclusions.

A great number of attempts, from purely empirical to semi empirical models have been made to predict the kinetics of ferrite transformation [28,29]. However, models

recently developed are becoming less empirical since they rely on thermodynamic and phase transformation theories [30]. Unemoto et. al. [31] developed a methodology to stimulate the alliomorphic ferrite transformation under isothermal conditions. Reed and Bhadeshia [32] reported a thermodynamic model coupled with a simplified kinetic theory. This model can reproduce the C-curve behavior typical of those parts of the TTT diagrams that are due to alliotromorphic ferrite in low carbon multi component steel. In principle, most of these are able to predict the kinetics of alliotromorphic ferrite for low carbon low alloy steels. But, the level of agreements between predicted and calculated alliomorphic ferrite kinetics is less satisfactory for medium carbon microalloyed steels.

On the other hand, it is well established that idiomorphic and acicular ferrite are the microstructures that improve the strength and particularly the toughness of steels. There is a large amount of works on acicular ferrite formation [33], but idiomorphic ferrite formation has been rarely studied. Some studies reported that idiomorphs might nucleate at precipitates of titanium oxide (Ti_2O_3), manganese sulphide (MnS), and vanadium nitride (VN). Those studies analyzed the reason for which such precipitates act as viable sites for intragranular ferrite nucleation, but the nucleation and growth kinetics for idiomorphic ferrite formation were not investigated. Furthermore, recent works have studied the role of the allotriomorphic ferrite to promote the formation of acicular ferrite to the detriment of bainite [34]. Thus, the amount of acicular ferrite increases by the presence of allotriomorphic ferrite along the austenite grain boundaries and/or the reduction of the amount of ferrite intragranularly nucleated on inclusions (idiomorphic ferrite). Therefore, a deep understanding of the decomposition of austenite in allotriomorphic and idiomorphic ferrite is needed in order to control the total amount of acicular ferrite in the microstructure.

2.6 Mechanical properties of HSLA steels

Blarasin and Farsetti (1989) [35] tested five microalloyed steels containing V, Nb and/or Ni in the carbon range of 0.21 to 0.41 wt.% for tensile and impact properties. Yield strength varies from 590 to 840 MPa and UTS from 800 to 940 MPa. Romm temperature impact energy was reported to lie in the range of 80 to 140 Jcm^{-2}. AISI 1141 vanadium microalloyed medium carbon steel in the as-forged condition has a yield strength (0.2% offset) of 524 MPa and tensile strength of 875 MPa [36]. Low carbon V/Nb microalloyed steels have been reported to have slightly higher compressive yield stress than the tensile value [37]. Compressive yield strength of the four steels studied was found to lie in the range of 450-610 MPa. HSLA steels also have lower ductile to brittle transition temperature. Typically a Charpy V-notch fracture appearance transition temperature of –40°C is achieved. Conventional controlled rolling can give excellent combination of strength (yield strength 450-525 MPa) and toughness (ITT as low as –80°C). ITT of low carbon ferrite-pearlite microstructure given by Glandman and Pickering, (1983) as:

$$ITT\ (^{\circ}C) = -19 + 44 * (wt.\%\ Si) + 700 * (wt.\%\ N_{free})^{1/2} + 2.2(\%\ pearlite) - 11.5d^{-1/2}$$

CHAPTER 3

EXPERIMENTAL PROCEDURE

3.1 Material for the present investigation

The chemical composition of medium carbon microalloyed forging grade steel (38MnSiVS6) used in this investigation is as given in Table 3.1. The steel supplied by Tata Iron and Steel Company, Jamshedpur, India in the form of 65RCS billet and was processed into required dimension (11 x 21 x 65) as shown in Fig. 3.1.

Table 3.1. Chemical composition of steel used in the investigation (wt.%).

Steel Grade	C	Si	Mn	P	S	V	N	Cr	Fe
38MnSiVS6	0.38	0.68	1.5	0.022	0.06	0.11	0.006	0.18	Bal.

3.2 Thermo-mechanical treatment

Hot rolling process followed by cooling tests were carried out on a laboratory 2-high rolling mill with 135mm diameter rolls and rolling speed of 55 rpm. In the present work, samples (11x 21x 65 mm) were reheated in a specially designed calibrated high temperature furnace, kept very close to the rolling mill to avoid much heat loss and were rolled to 3.5mm thick plates with three different rolling schedules. No prior heating of the rolls were done before hot rolling of the specimens and they were maintained at room temperature. The inert argon atmosphere was maintained inside the furnace to prevent oxidation of steel while heating and soaking. The sample temperature was measured by calibrated radiation pyrometer.

The flow chart and schematic representation of thermo-mechanical treatment given is as shown in Figs. 3.2 and 3.3, respectively. All the thermomechanical schedules involved reheating the steel to austenitizing temperature, soaking for 30minutes and rolled to finish rolling temperatures of (i) 850 to 900°C(i.e., above Ar_3 temperature), (ii) 800 to 850°C (i.e., at Ar_3 temperature) and 750 to 800°C (i.e., below Ar_3 temperature).

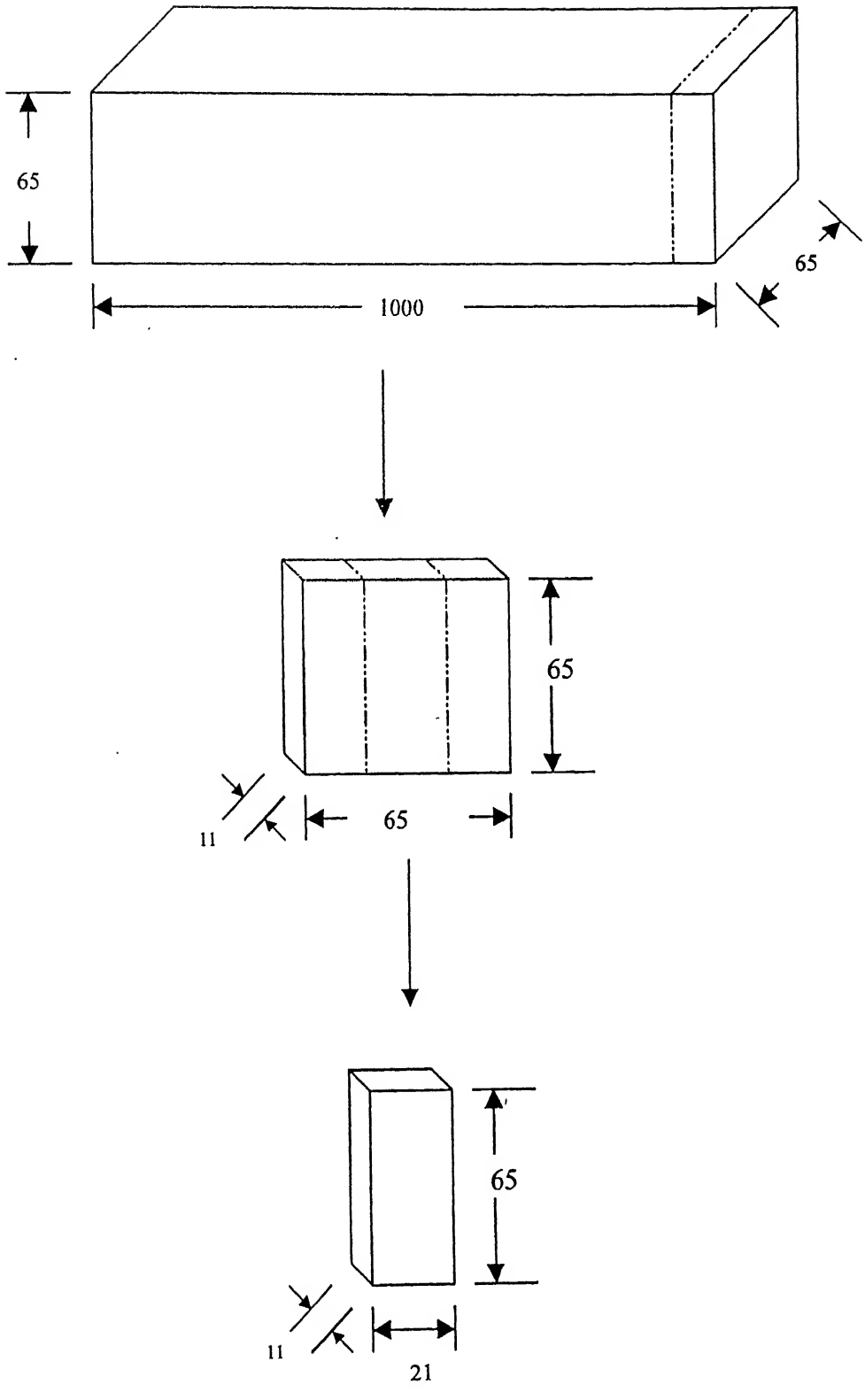

Fig. 3.1: Flow diagram of processed of processed sample into required dimensions (All dimensions in mm).

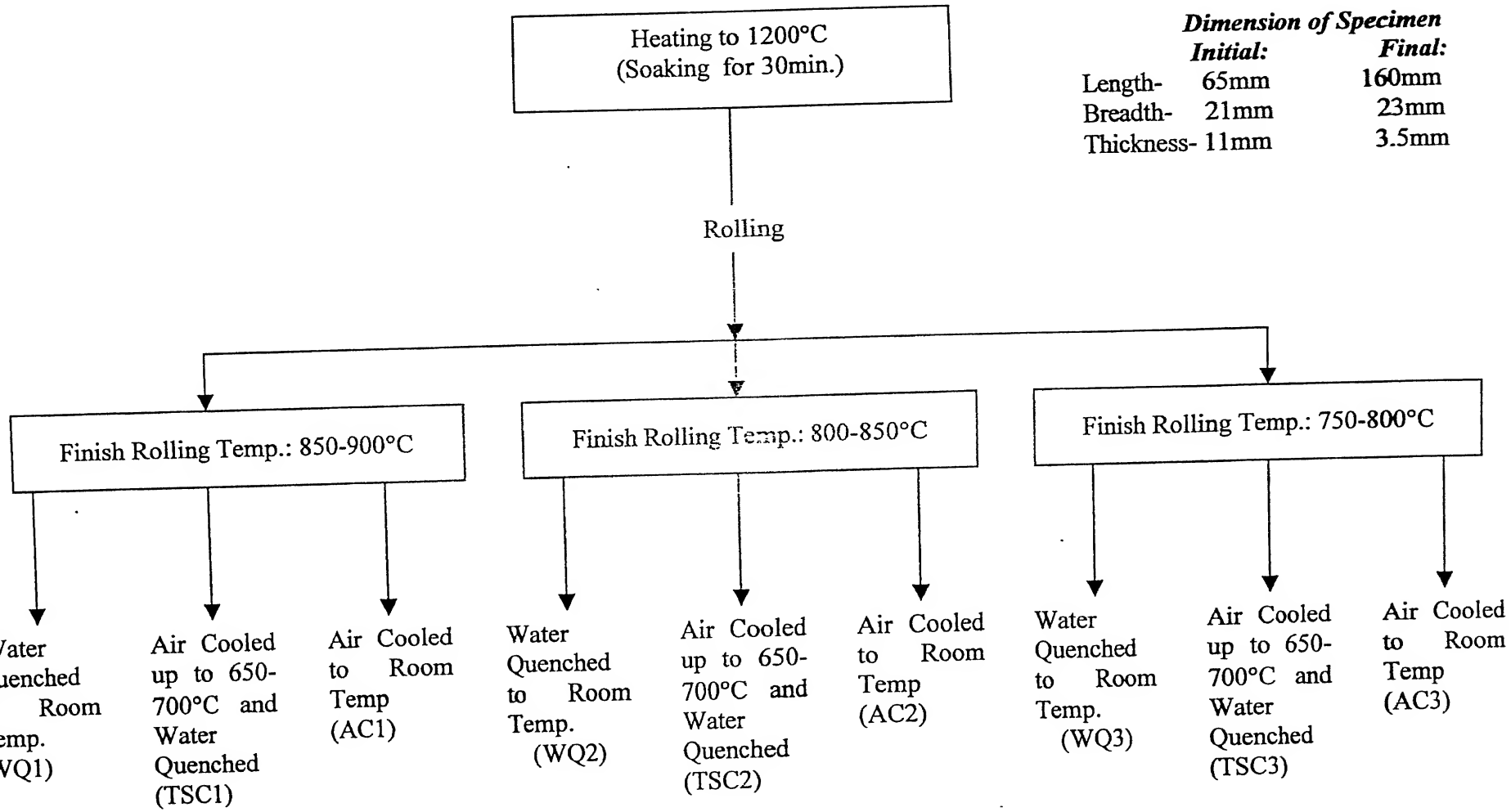

Fig 3.2. Thermomechanical treatment given to 38MnSiVS6

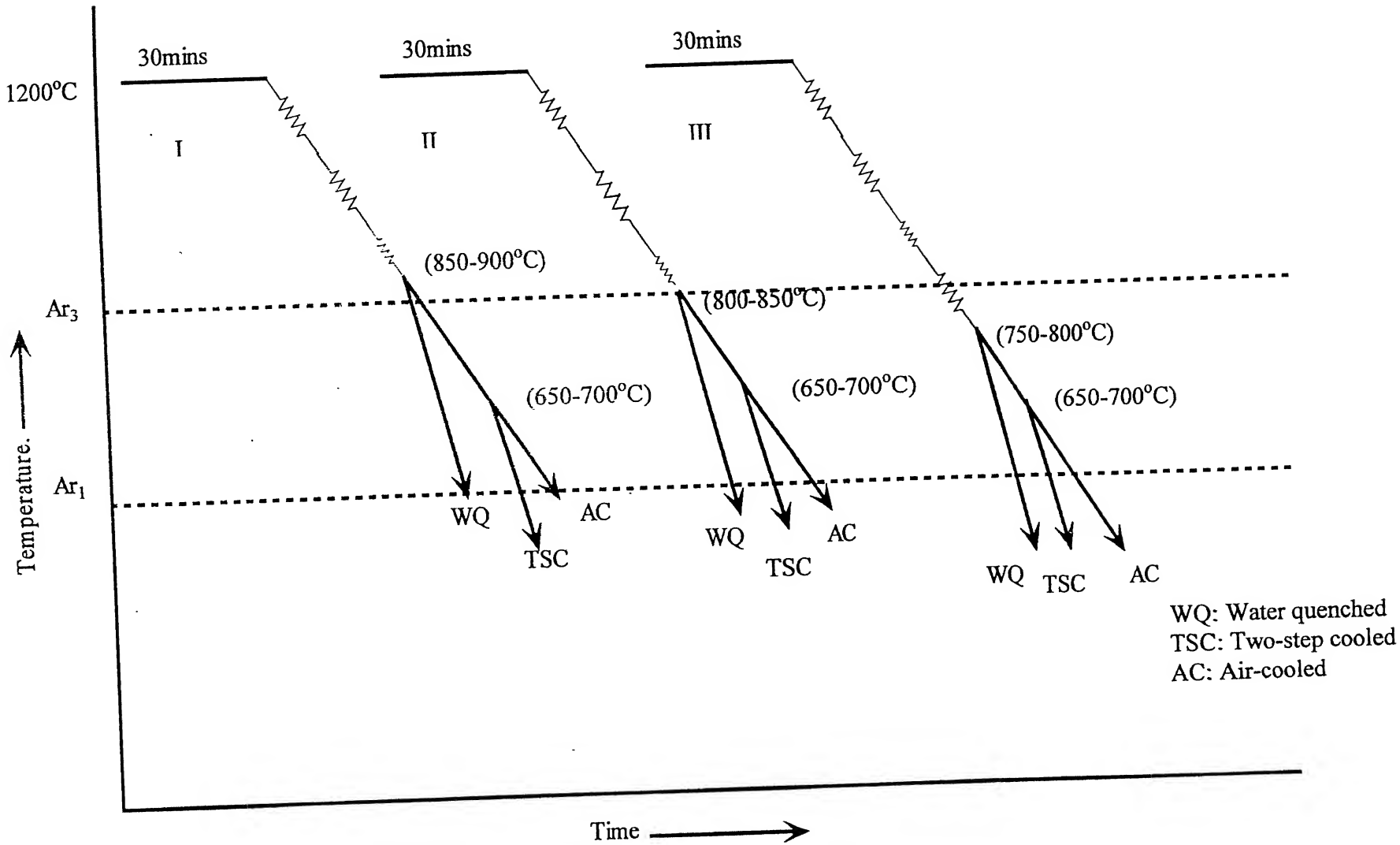

Fig.3.3: Schematic representation of rolling schedule

(I- schedule1; II- schedule2; III- schedule3)

The rolled samples were subsequently subjected to three different cooling rates: (i) air-cooling (AC), (ii) two step cooling (TSC) and (iii) water quenching (WQ). Three samples for each route were taken. Here total % reduction was kept constant and the only differences between these schedules were the finish rolling temperature. No annealing treatment was given, so as to analyze the change after thermo mechanical treatment.

In order to study the effect of deformation start temperature on microstructure, the thermomechanical treatment selected is shown in Fig. 3.4. Here the above steel was heated to T_d (1200, 1150, 1100, 1050 and 1000°C), soaked for 30mins and rolled with four passes followed by final air-cooling. Three samples were taken for each treatment. The % reduction in thickness and 2mins soaking time after each pass was kept constant, so that only variable was deformation start temperature. The fall in temperature after deformation was 100 to 150°C in every treatment.

In order to measure prior austenite grain size the steel was heated to T_d, soaked for 30 minutes and water quenched in order to restrain grain growth during cooling. The flow chart is as shown in Fig. 3.5.

3.3 Microstructural characterization

3.3.1 Sample preparation and optical microscopy

The microstructure samples were cut from the shoulder of tensile samples by using abrasive cutter perpendicular to rolling direction and mounted by hot mounting process. The mounted samples were ground using a belt grinder followed by polishing on emery paper of various grades (1 to 4 grades). The paper polished samples were then wheel polished. Alumna powder of 0.5μm was used for wheel polishing. The mirrors like polished samples were etched using three different etchent [38] depending upon the treatment.

T_d °C: 1200,1150,1100,1050,1000

Sample Dimensions:

	Initial	Final
Length-	65mm	160mm
Breadth-	21mm	23mm
Thickness-	11mm	3.5mm

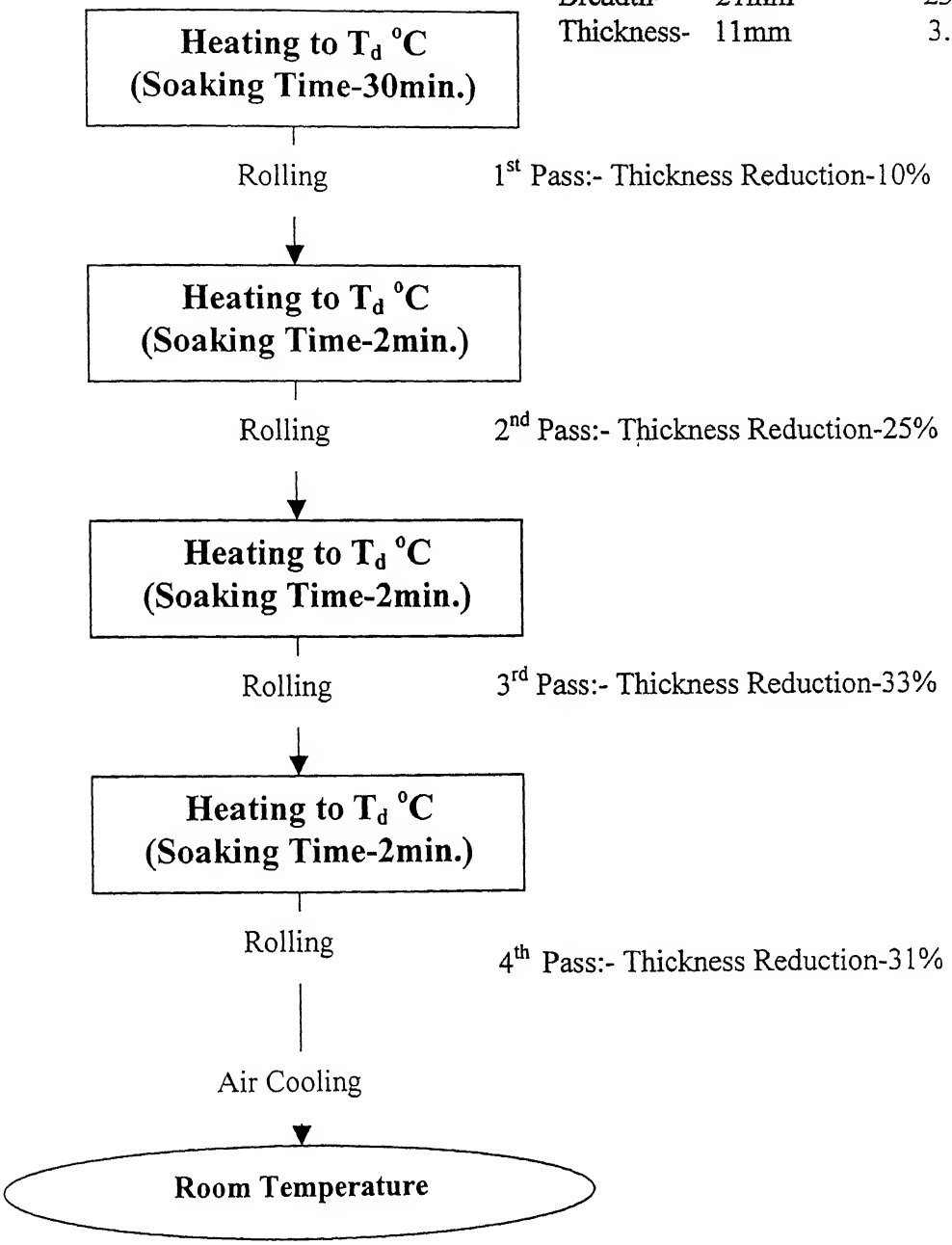

Fig.3.4: Flow diagram to study effect of deformation start temperature

T_d °C:
1200,1150,1100,1050,1000

Sample Dimensions:
Length- 65mm
Breadth- 21mm
Thickness- 11mm

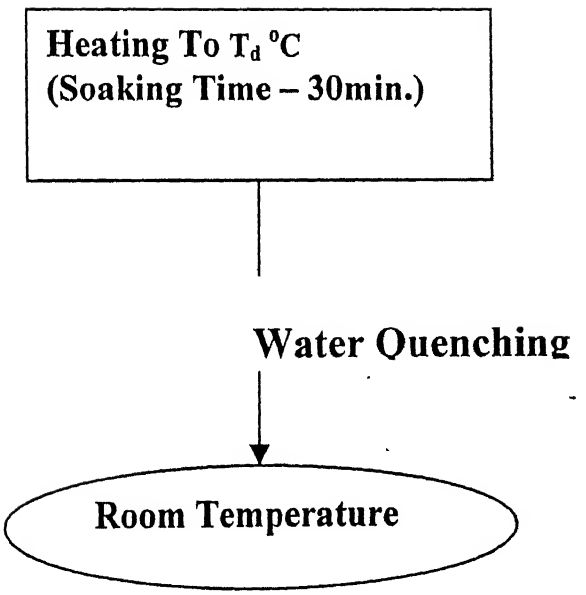

Fig. 3.5: Flow Diagram to study prior austenite grain size

1. Etchent 1: 2% Nital solution (2 ml HNO_3 + 98 ml Ethanol), etch time 20 to 25sec: general purpose etchent to reveal various phases.
2. Etchent 2: Sat. aq. Picric acid (2gm picric acid in 100ml water and one tea spoon Teepol as wetting agent), etch time 20 to 30mins to reveal prior austenite grain boundaries in steel.
3. Etchent 3: A solution of 1g sodium metabisulfite and 100ml water, mixing in equal proportion of 4gm picric acid and 100ml ethanol, etch time 7 to 12 sec to distinguish ferrite, bainite and martensite.

Leize wetzler optical microscope was used for low magnification microstructural study. The prepared samples were observed under the magnification of 100X, 200X and 500X. Jenavert carl zeiss optical microscope was also used to study the microstructure at magnification 1600X. However, this magnification was insufficient to measure interlamellar spacing of pearlite. Microstructural study was done transverse to the rolling direction. At these magnifications the morphology of phases were conveniently studied.

3.3.2 Stereological Measurements

Axiolab zeiss optical microscope with a maximum magnification of 500X, connected to a computer by video input device, was used to acquire microstructural images. Image-pro plus imaging software tool was used for stereological measurements. The captured images were subjected to image processing, as shown in Fig 3.6. Fig. 3.6a is the captured image from the sample at 200X and Fig. 3.6b is the processed image by gamma correction (a specialized form of contrast enhancement). The stereological parameters selected for measurements are described below.

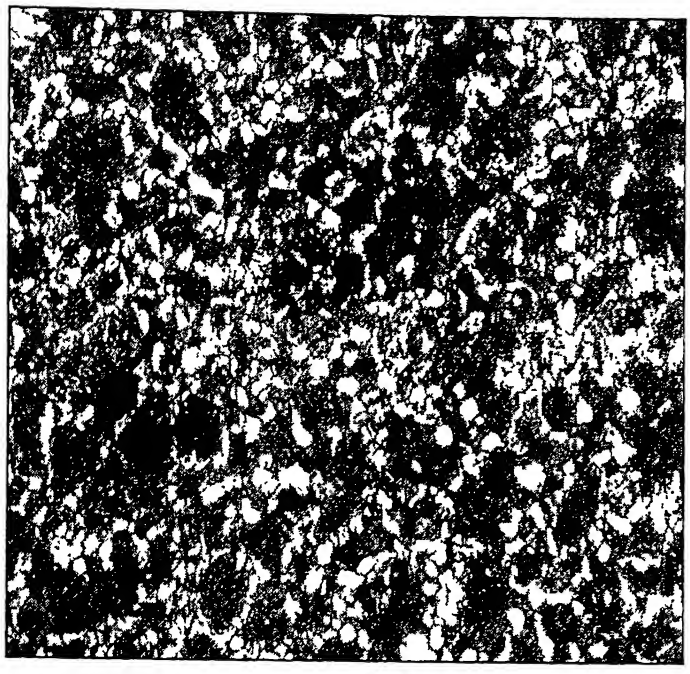

(a)

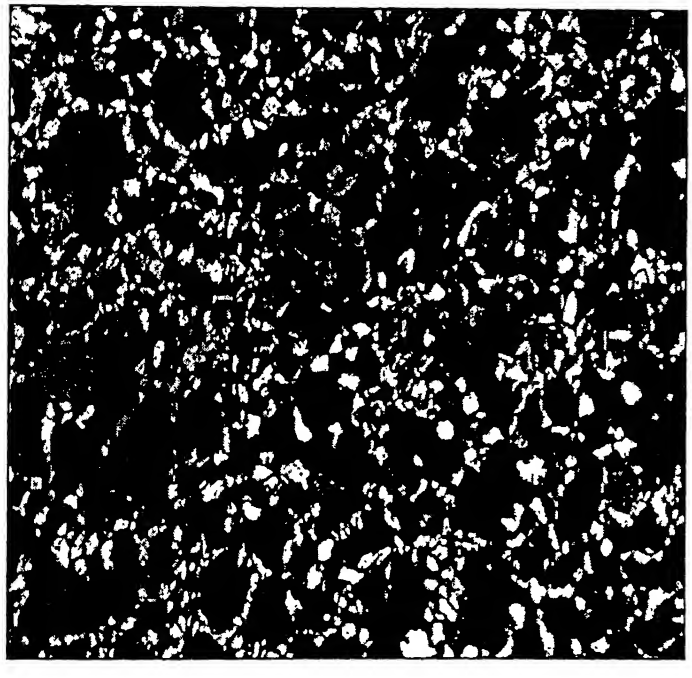

(b)

Fig3.6: Micrograph of Air-cooled sample

(a) Before image processing.
(b) After gamma correction.

The volume fraction of α phase was equated to areal fraction as:

$$(V_V)_\alpha=(A_A)_\alpha \qquad \text{.....(3.1)}$$

where $(A_A)_\alpha$ is the sum of areas of α phase divided by total test area.

For the measurement of grain size the linear intercept method was used by putting the grid lines (3 horizontal and 1 vertical) of total length 621.249μm (L_T) at 100X or 200X using image-pro plus software.

For single-phase structure, the mean intercept length ($\overline{L_3}$) is given by the following relationships:

$$\overline{L_3}=\frac{1}{P_L} \qquad \text{.....3.2)}$$

For two phase structure (consisting of ferrite and pearlite), the mean intercept length ($\overline{L_3}$) of pearlite colony is given by the following relationships:

$$\overline{L_3}=\frac{2V_V}{P_L} \qquad \text{.....3.3)}$$

where P_L is the number of point intersections per unit length of test lines with ferrite–pearlite boundaries.

V_V is the volume fraction of pearlite.

To ensure that measurements were representative of the structure, 25 fields were selected randomly to avoid any bias. The average of these values are accounted per sample and statistical analysis (95% confidence limit) of these samples were done. The counting of intersection points was done manually.

The 95% confidence limit (CL) is calculated using the following relationship;

$$95\%\ CL=\left(\frac{2s}{(N-1)^{1/2}}\right) \qquad \text{.....3.4)}$$

where 's' is standard deviations of data and 'N' is the number of measurement.

3.4 Tensile testing

Tensile specimens were prepared according to ASTM standard as shown in Fig. 3.7. The tensile specimen was prepared carefully to avoid the notch effect. From the rolled material of ~3.5 mm thickness it was not possible to prepare Charpy/Izod samples for toughness testing or the notched samples for K_{Ic} value determination. Tensile tests were done at a strain rate of 10^{-4}/sec in strain control mode using a closed loop servo-hydraulic material testing machine. The ultimate strength (UTS) and yield strength (YS) were calculated from the stress-strain curves. The toughness (U_T) was approximated by the following expression [39]:

$$U_T \approx \left(\frac{S_o + S_u}{2}\right) e_f \qquad \text{.....3.5)}$$

where S_o is 0.2% offset yield strength, S_u is ultimate tensile strength and e_f is engineering strain at fracture

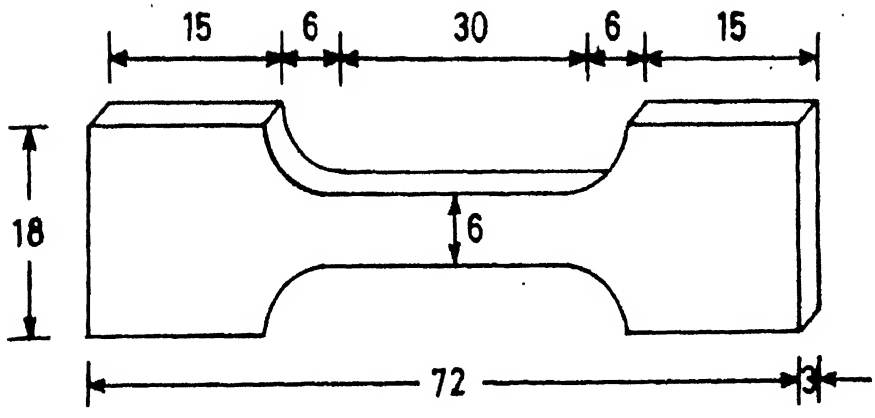

All dimensions in mm

Fig. 3.7: Tensile test specimen

1

CHAPTER 4

RESULT AND DISCUSSIONS

The microstructures of thermomechanically treated 38MnSiVS6 microalloyed samples thus obtained were characterized by various techniques, already discussed in chapter 3. Similarly, the mechanical properties of each treatment were measured. Results obtained on them have been described and discussed in the present chapter.

4.1 Structure of as received 65RCS billet:

The microstructure of as received steel sample, shown in Fig.4.1, reveals a typical pearlite-ferrite structure. % Volume fraction and aspect ratio of ferrite were automatically measured using image analyzing software and was found to be 20.10, and 1.61, respectively. The pearlite colony size, measured by the linear intercept method for two-phase structure (equation 3.3), was found to be 31.03μm.

4.2 Effect of deformation start temperature on 38MnSiVS6 steel

An attempt was made to study the effect of deformation start temperature on grain size and ferrite morphology by subjecting the samples to the thermomechanical treatment given in Fig. 3.4. Fig.4.2 shows the microstructures corresponding to deformation start temperature (T_d) 1000, 1050, 1100, 1150 and 1200°C. The micrographs at higher magnifications are shown in Figs. 4.3 (a) and (b), respectively. Since the cooling rate is slow (air cooled) the microstructures obtained are mixture of ferrite and pearlite. Fig. 4.4 shows the prior austenite grain boundaries (PAGB) at a magnification of 100X. The measured quantities are tabulated as in Table 4.1.

The effect of deformation temperature on grain size is shown in Fig.4.5 (a). Nucleation of proeutectoid ferrite occurs at the austenite grain boundaries, so the pearlite colony size measures the austenite grain size after deformation. Prior austenite grain size before deformation and pearlite colony size after deformation increases with the temperature, the difference is maximum at 1200°C because of maximum dynamic

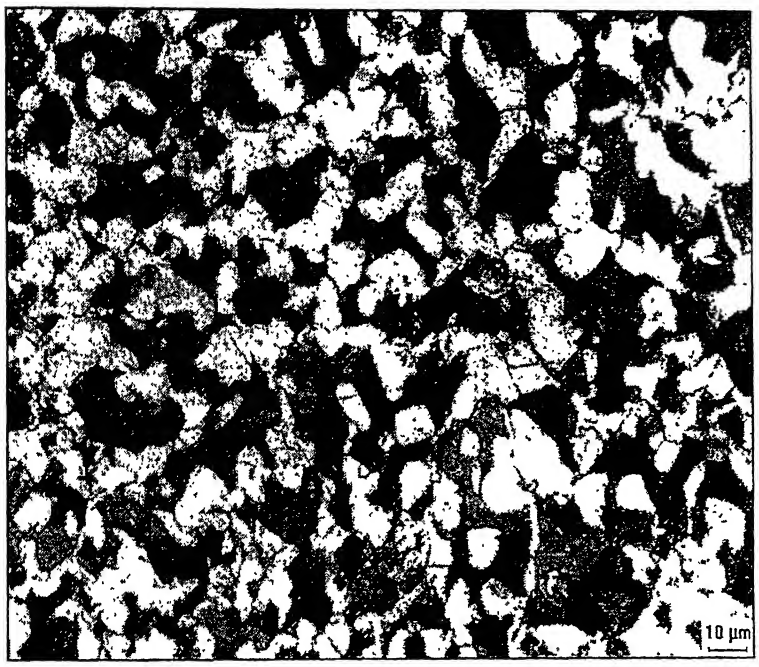

Fig.4.1: Micrograph of as received material at 200X

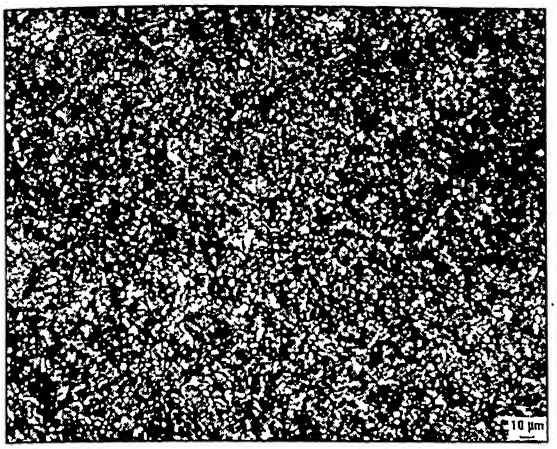

(a)

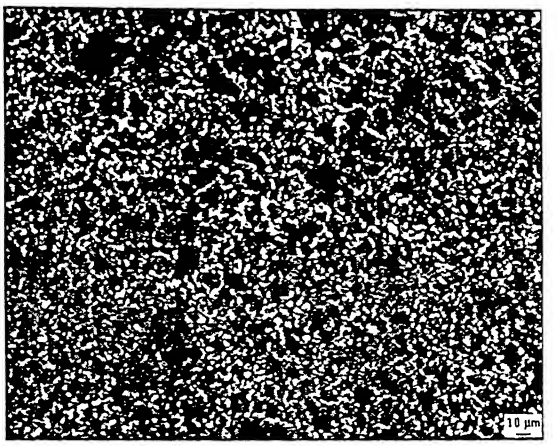

(b)

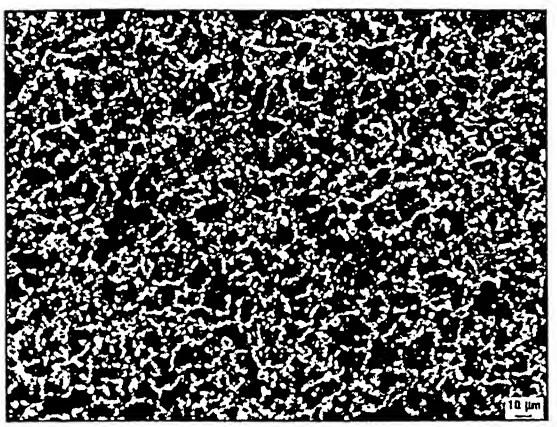

(c)

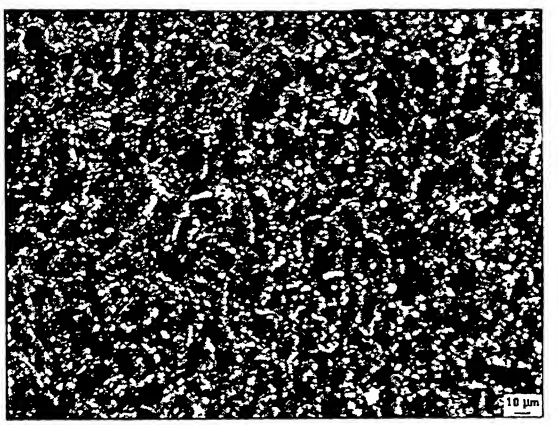

(d)

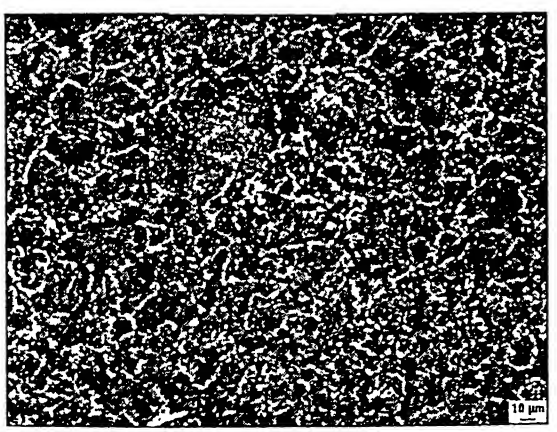

(e)

Fig.4.2: Microstructures at magnification 100X for samples rolled at deformation start temperature (a) 1000°C (b) 1050°C (c) 1100°C (d) 1150°C & (e) 1200°C

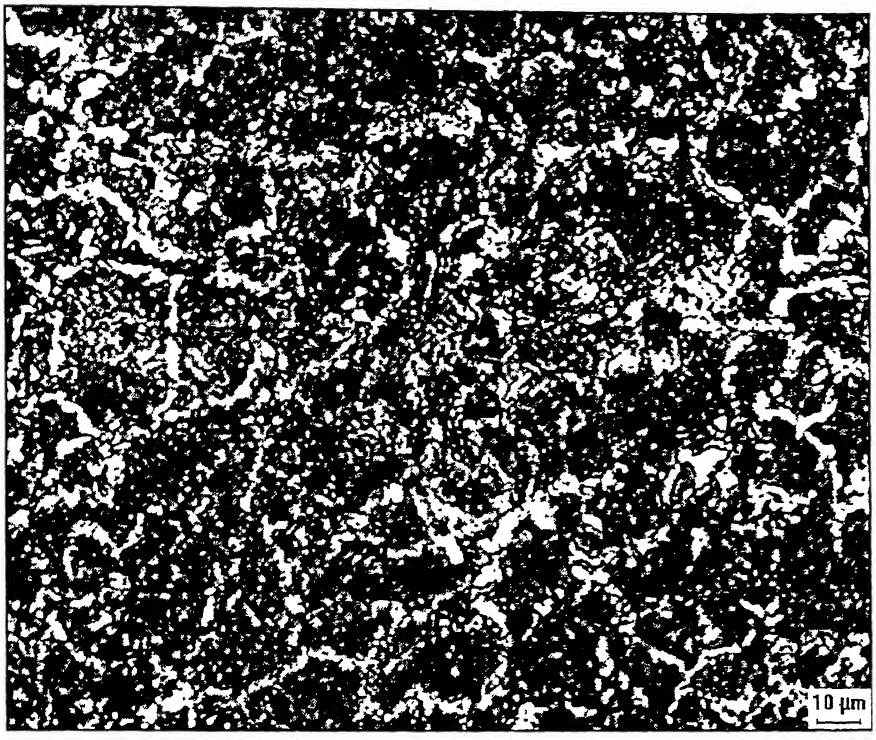

(a)

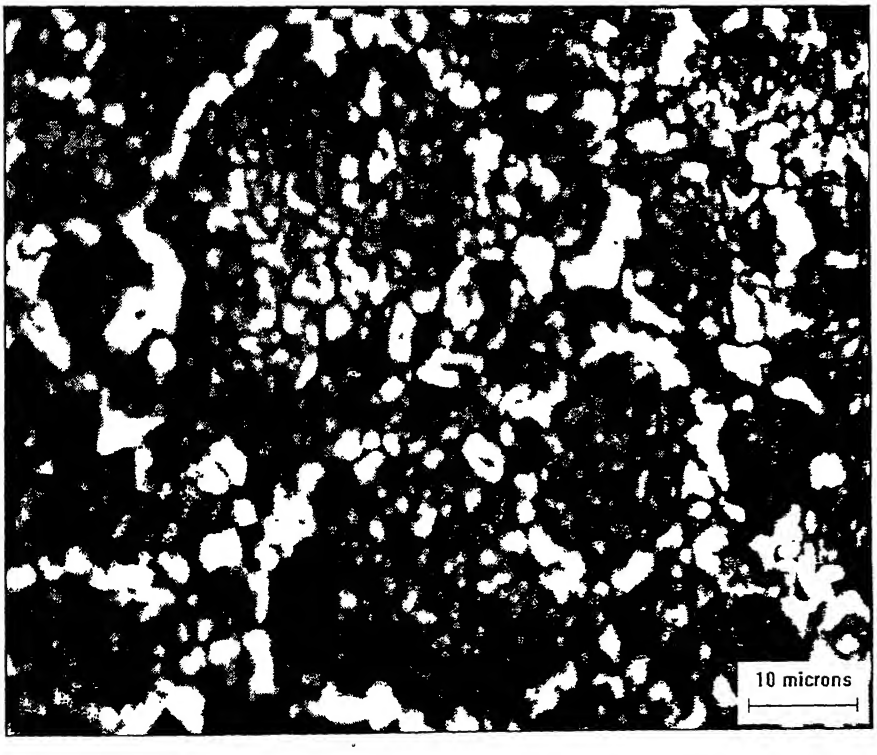

(b)

Fig.4.3: Higher magnification micrographs to study deformation start temperature: (a) 200X and (b) 500X

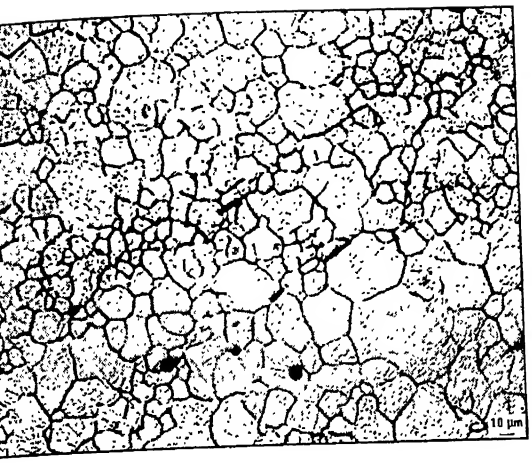

(a)

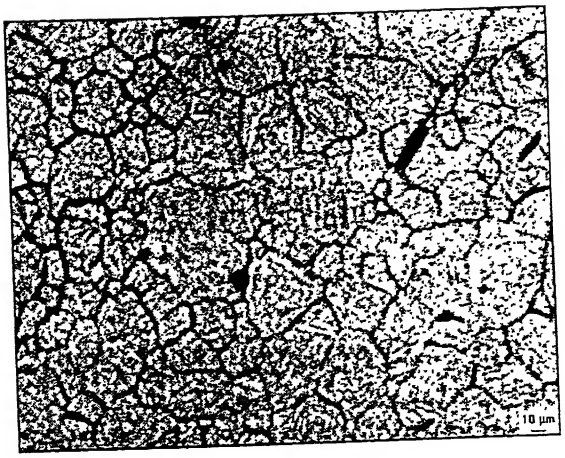

(b)

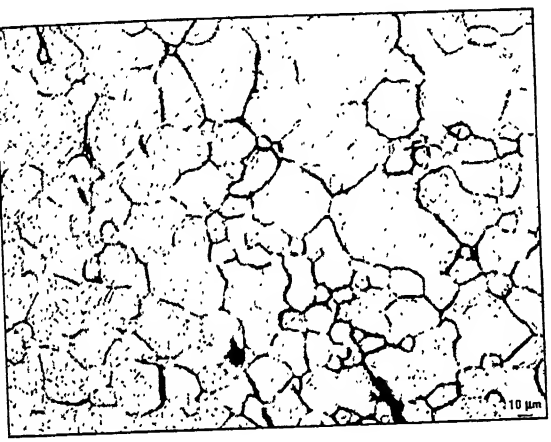

(c)

(d)

(e)

Fig.4.4: Prior austenite grains for deformation start temperature of (a) 1000°C (b) 1050°C (c) 1100°C (d) 1150°C & (e) 1200°C. Magnification: 100X

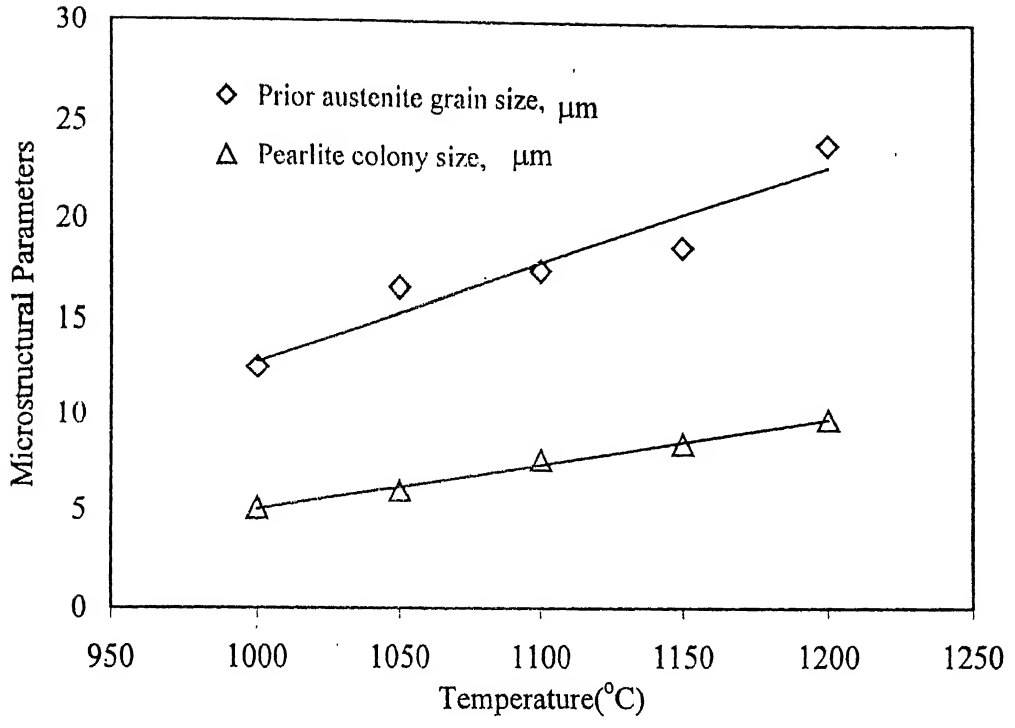

(a)

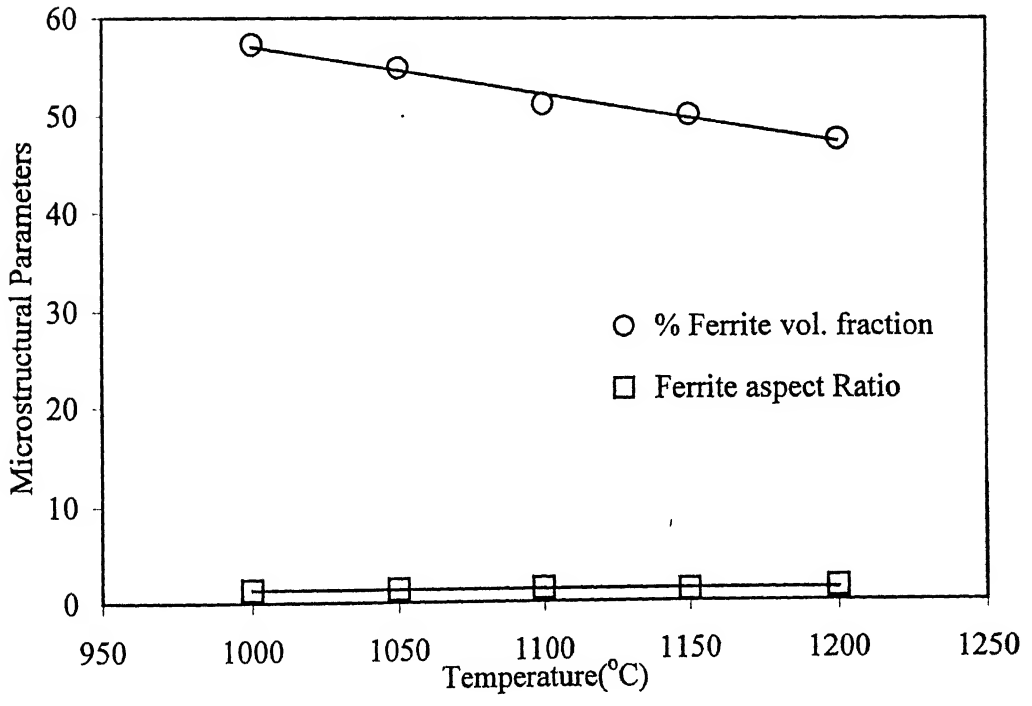

(b)

Fig 4.5:Variation of microstructural parameters as a function of deformation start temperature

recrystallization and complete solid solubility of vanadium, resulting in precipitation of VC/V(CN) along the grain boundaries, which obstructs the grain boundary migration on cooling. As shown in Fig.4.5 (b) the volume fraction of ferrite decreases with the increase of T_d because of increase in grain size i.e. effective grain boundary area per unit volume of austenite decreases. The grain boundaries are preferential sites for ferrite nucleation and also the VC/V(CN) precipitates are undissolved at lower temperature, so the effective carbon in austenite is low, resulting in higher volume fraction of ferrite at the low deformation temperature. It is noted that there is not much change in aspect ratio of ferrite as the deformation temperature changes. At 1000 and 1050°C the idiomorphic ferrite is present, which can be clearly seen in Fig. 4.3. This is due to the dislocation as the preferential site for ferrite nucleation and extend is maximum at 1000°C, i.e. deformation is below dynamic recrystallization temperature.

The complete dissolution of VC/V(CN) precipitates with maximum dynamic recrystallization at 1200°C , resulting in minimum volume fraction of ferrite as compared to lower deformation temperature. So, deformation start temperature of 1200°C is chosen for subsequent thermo-mechanical treatments.

T_d °C	*PAG	AFTER DEFORMATION		
	PAG size, $\overline{L_3}$ (μm)	**Pearlite colony size, $\overline{L_3}$ (μm)**	**Ferrite vol. fraction, V_V (%)**	**Ferrite aspect ratio**
1200	24.005	9.8241	47.5	1.41
1150	18.662	8.5292	50.07	1.16
1100	17.43	7.6979	51.18	1.35
1050	16.578	6.014	54.91	1.31
1000	12.532	5.0686	57.33	1.29

* Prior Austenite Grain

Table 4.1: Variation of the measured quantities with T_d.

T_d °C	*PAG	AFTER DEFORMATION		
	95% CL of P_L (%)	95% CL of P_L, pearlite (%)	95% CL of ferrite vol. fraction (%)	95% CL of ferrite aspect ratio (%)
1200	1.42	2.44	0.87	.033
1150	2.4	8.5292	1.26	0.06
1100	1.73	7.6979	0.75	0.03
1050	2.06	6.014	1.78	0.04
1000	1.74	5.0686	1.59	0.02

Table 4.2: 95% confidence limit values of measured data's for deformation start temperature study.

4.3 Microstructures of thermo-mechanically treated 38MnSiVS6 plate

4.3.1 Microstructure of air-cooled samples.

Fig 4.6 shows the effect of rolling finish temperature on the microstructure of air-cooled samples for three different schedules. Figs. 4.6(a) and (b) are the micrographs of AC1 at 200X and 500X magnification, respectively, shows the polymorphic ferrite with matrix of pearlite. Figs. 4.6 (c) and (d) are the micrograph of AC2 at 200X and 500X, having mixture of polymorphic ferrite and pearlite, similarly Figs. 4.6 (e) and (f) are the micrograph of AC3 at 200X and 500X, respectively, having both idiomorphic and polymorphic ferrite with pearlite matrix. The pearlite lamellae for air-cooled samples were resolved at 1600X magnification, as in Fig 4.7. Figs.4.8 (a) and (b) shows the effect of using etchents 1 and 3 (refer section 3.3.1), respectively on air-cooled sample with dark phase as pearlite and white as ferrite [38]. As can be seen, the two etchents for air-cooled samples reveals more or less same phases.

The measured quantities %ferrite volume fraction, ferrite aspect ratio and pearlite colony size are tabulated for air-cooled samples as in Table 4.3.

4.3.2 Microstructure of two-step cooled samples (TSC)

The effect of TSC (see Fig: 3.3) on microstructure and tensile properties were studied. Figs. 4.9(a) and (b) shows the micrograph of TSC1 samples at magnifications 200X and 500X respectively. The microstructure reveals proeutectoid ferrite and martensite. Figs. 4.9 (c) and (d) are the micrographs of TSC2 samples at 200X and 500X magnifications having proeutectoid ferrite along the boundaries of martensite matrix. Figs. 4.9 (e) and (f) are the micrograph of TCS3 sample at 200X and 500X respectively, with similar morphology of ferrite and martensite with higher volume fraction of ferrite.

At a magnification of 1600X (in Fig.4.10) and by the use of etchant3 (as in Fig.4.8) it is clearly seen that, matrix is martensite. The measured microstructural parameters are tabulated as in table.4.3.

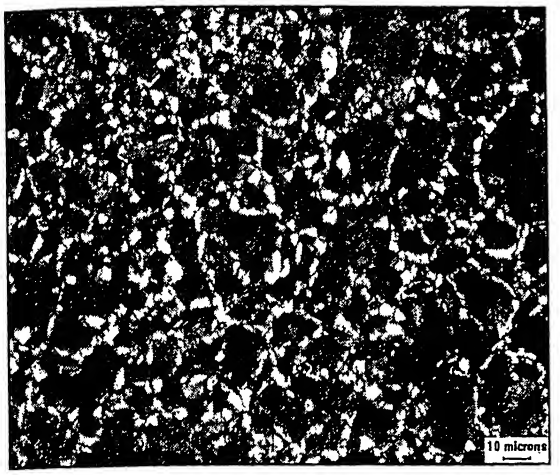

(a)

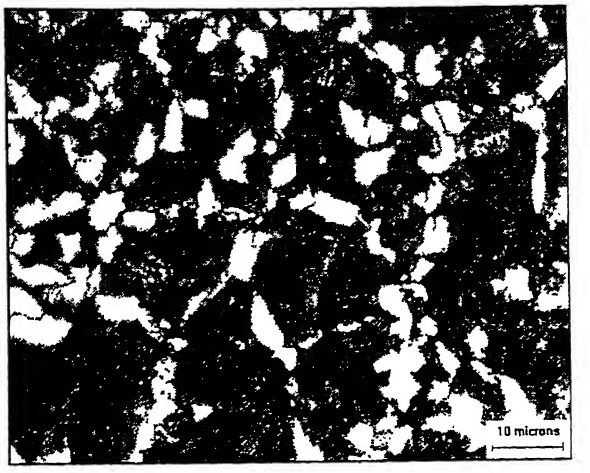

(b)

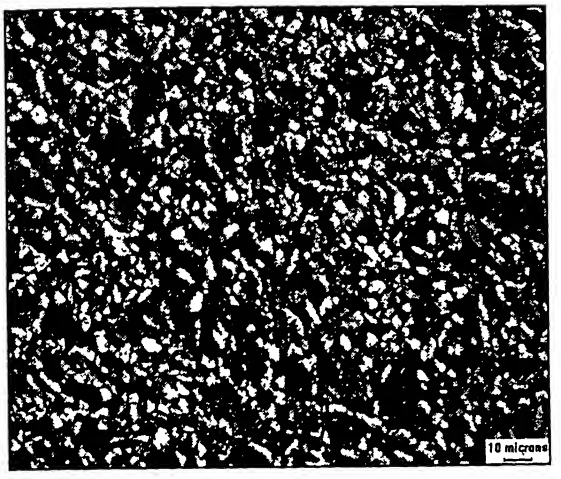

(c)

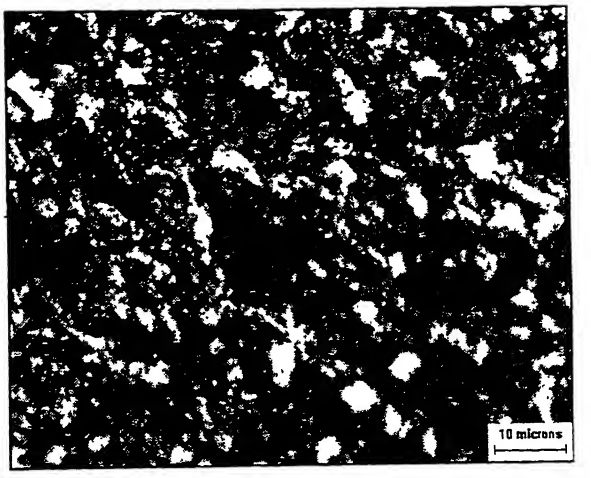

(d)

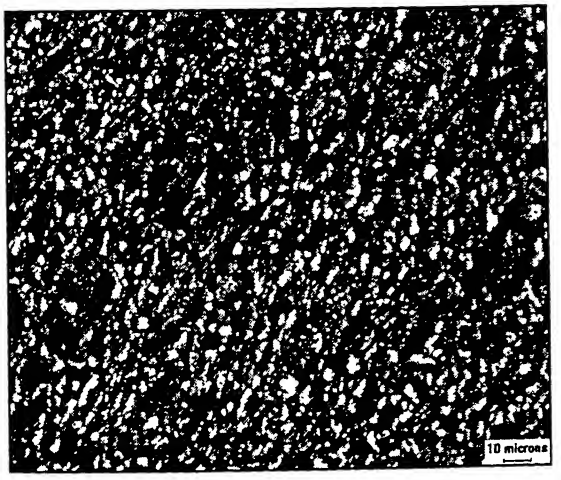

(e)

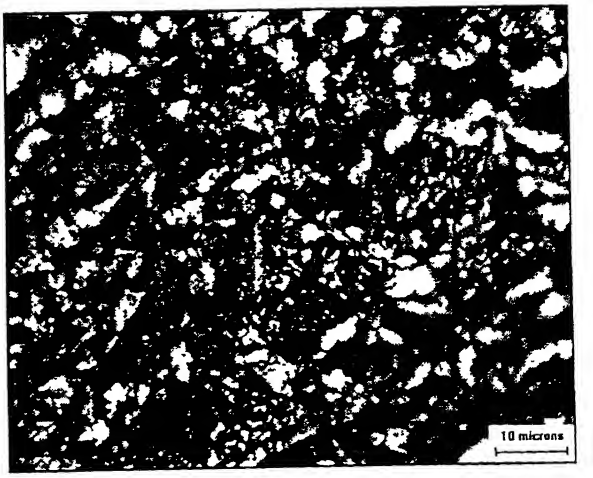

(f)

Fig. 4.6: Micrograph of air-cooled samples (a) & (b) AC1 at 200X & 500X, (c) &(d) AC2 at 200X & 500X, (e) & (f) AC3 at 200X & 500X.

	AC1	AC2	AC3	TSC1	TSC2	TSC3
Ferrite volume fraction (%)	16.51	19.94	26.09	9.36	15.48	11.77
Ferrite aspect ratio	1.82	1.93	2.11	1.77	1.78	1.79
Pearlite colony size (μm)	18.54	16.82	13.03	-----	-----	-----
UTS (MPa)	975.5	888.68	966.59	1656.73	1424.33	1647.23
Yield strength (MPa)	746.4	683.45	808.73	1305.43	1128.18	1329.92
Toughness (MPa)	126.28	130	138.43	199.85	146.34	222.56

Table 4.3: Measured microstructural parameters and tensile properties in air-cooled and two-step cooled samples

	WQ1	WQ2	WQ3
Prior austenite grain size (μm)	10.07	9.63	8.93
UTS (MPa)	1947.69	1895.86	1914.59
Yield strength (MPa)	1716.72	1606.33	1684.85
Toughness (MPa)	299.43	273.24	273.15

Table 4.4: Measured microstructural parameters and tensile properties in water quenched samples

	AC1	AC2	AC3	TSC1	TSC2	TSC3
95% CL of %ferrite volume fraction (%)	0.81	1.56	1.54	1.01	1.42	1.36
95% CL of ferrite aspect ratio (%)	0.02	0.021	0.05	0.015	0.018	0.015
95% CL of P_L, pearlite (%)	1.05	2.35	2.01	-----	-----	-----

Table 4.5: 95% confidence limit values of measured quantities for AC and TSC samples

	WQ1	WQ2	WQ3
95% CL of P_L, prior austenite grain (%)	0.56	0.95	0.87

Table 4.6: 95% confidence limit values of measured quantity for water quenched samples

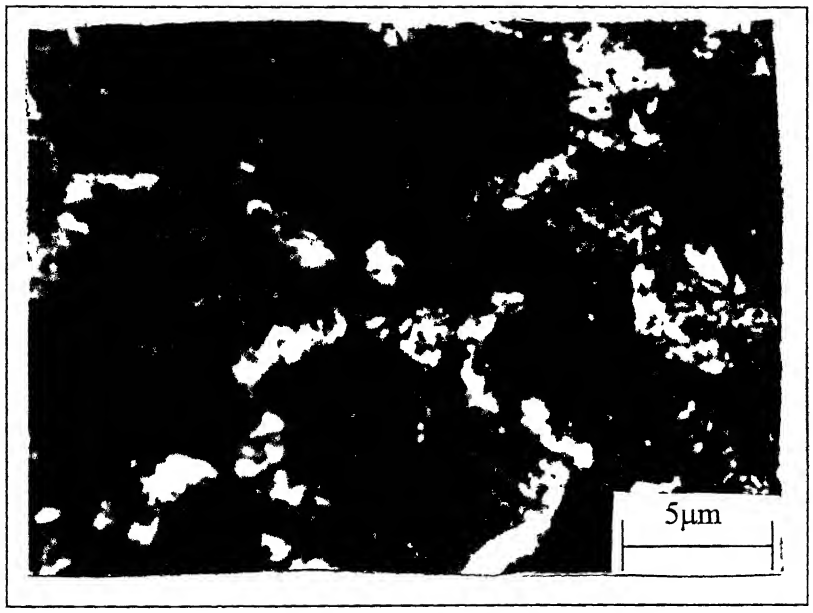

Fig.4.7: Higher magnification (1600X) micrograph for an air-cooled sample.

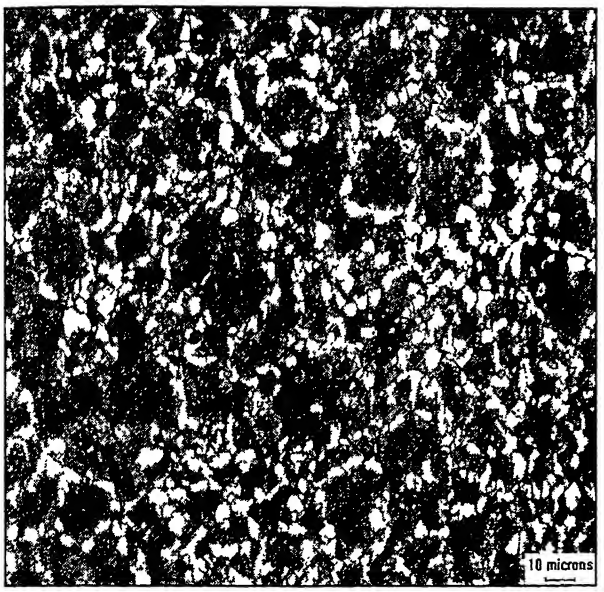

(a)

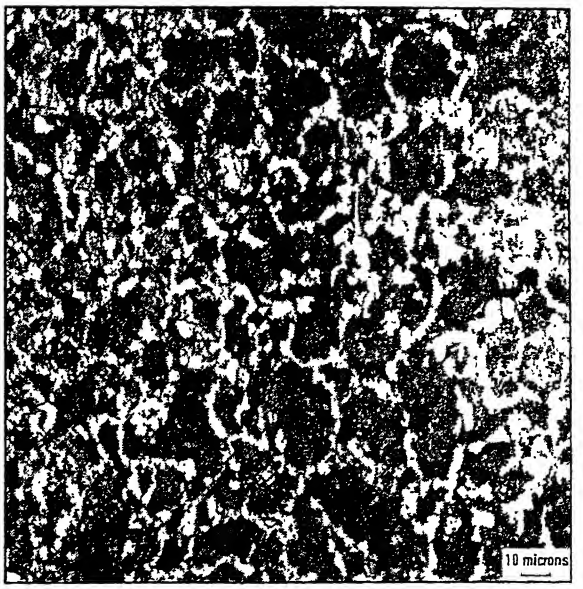

(b)

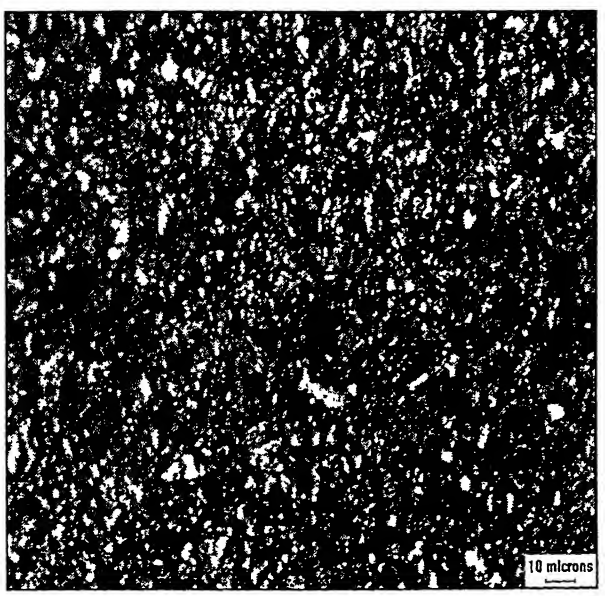

(c)

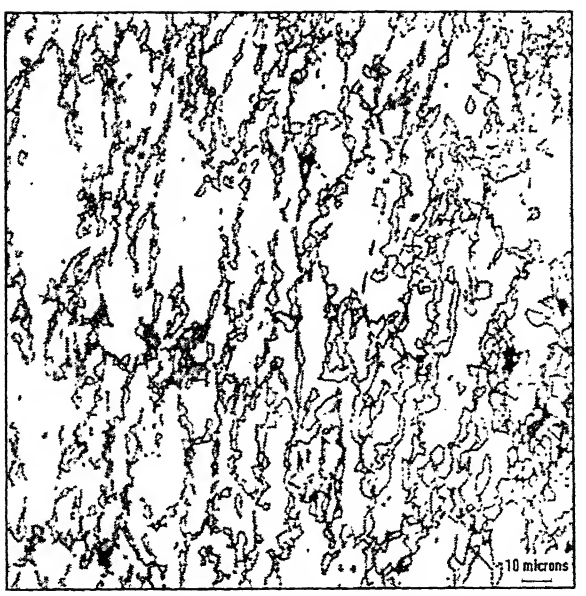

(d)

Fig. 4.8: Effect of using two different etchents on sample, (a) and (b) air cooled, (c) and (d) two step cooling

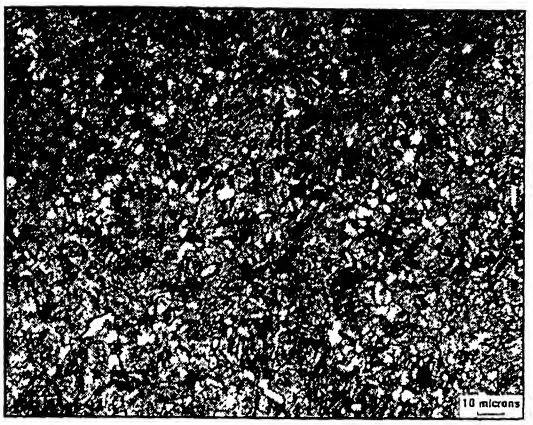

(a)

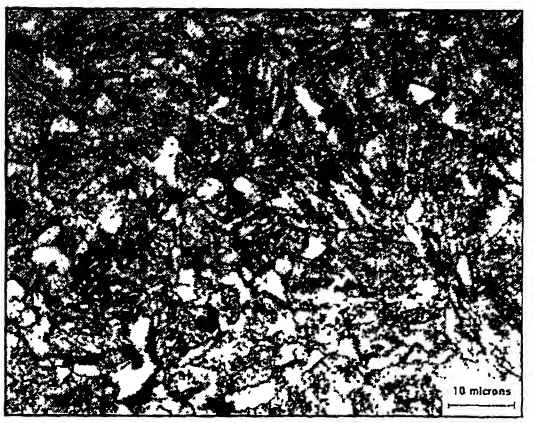

(b)

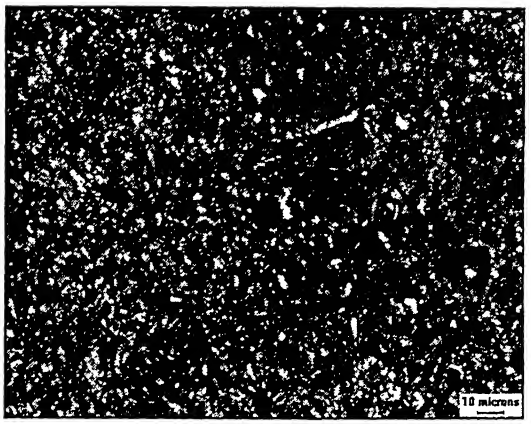

(c)

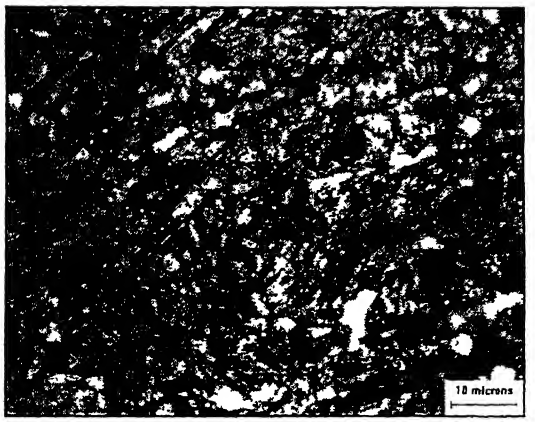

(d)

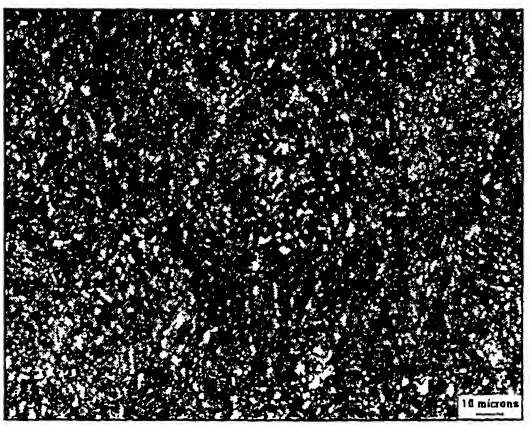

(e)

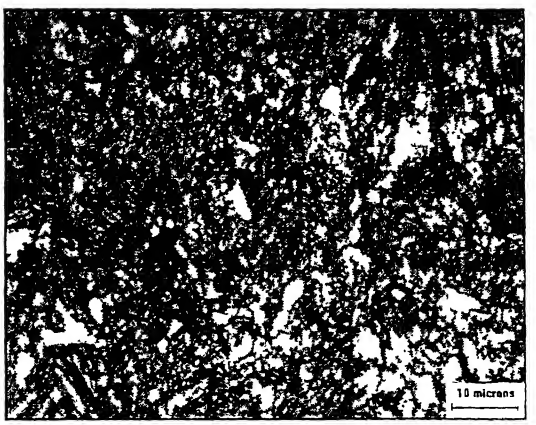

(f)

Fig. 4.9: Micrograph of two-step cooled samples (a) & (b) TSC1 at 200X & 500X, (c) &(d) TSC2 at 200X & 500X, (e) & (f) TSC3 at 200X & 500X.

Fig.4.10: Higher magnification (1600X) micrograph for a two-step cooled sample.

4.3.3 Microstructures of water quenched samples (WQ)

Figs. 4.11 (a), (b) and (c) are the micrographs of water quenched samples of WQ1, WQ2 and WQ3 schedules, respectively at magnifications of 500X. Microstructures reveal 100% martensite or martensite with little ferrite. However, the ferrite morphology could not be quantified. Fig. 4.12 shows the microstructure of water-quenched samples at 1600X.

Fig.4.13 shows the grain boundaries of above treated samples using etchant-3,used to measure the grain size as tabulated in Table4.4. The slightly elongated grains in the micrographs are due to the lateral spread of material during rolling, although the microstructure is seen transverse to the rolling direction. Fig.4.13(c) shows the nucleation of ferrite at the grain boundary because the rolling finish temperature is below the Ar_3 temperature line as shown in the schematic diagram (refer Fig. 3.3).

4.4 Tensile properties of thermo-mechanically treated 38MnSiVS6 steel plates

The tensile tests were performed to understand the effect of microstructural changes in 38MnSiVS6 steel on its various tensile properties at room temperature, viz. the yield strength, the ultimate tensile strength and the toughness. The tensile properties of the steel were obtained for the following thermomechanically treated samples (refer Fig. 3.3).

- Hot rolled and air cooled (AC) with three different rolling finish temperature: schedule I, schedule II & schedule III.
- Hot rolled and two-step cooled (TSC) with three different rolling finish temperature: schedule I, schedule II & schedule III.
- Hot rolled and water quenched (WQ) with three different rolling finish temperature: schedule I, schedule II & schedule III.

This section of the present chapter describes the results on yield strength, ultimate tensile strength and the toughness obtained from the flat tensile samples.

Yield strength:

Air cooled sample has clear yield point but for TSC and WQ samples 0.2% yield strength

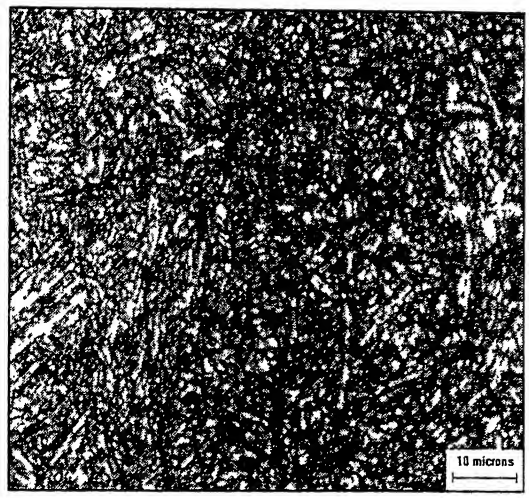

(a)

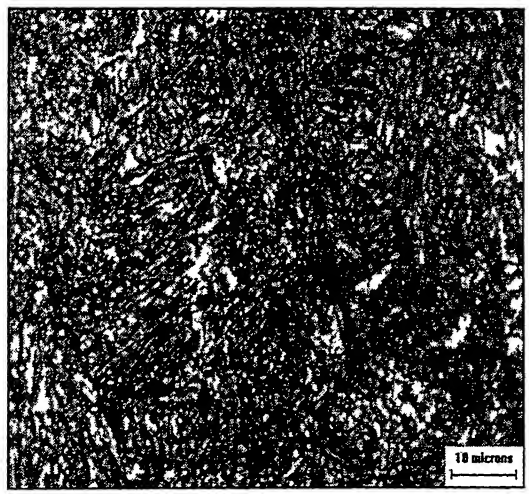

(b)

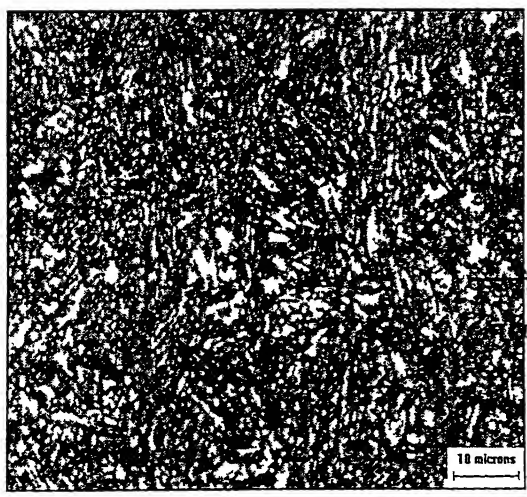

(c)

Fig.4.11: Micrograph of water quenched samples (a) WQ1, (b) WQ2 and (c) WQ3. Magnification: 500X

Fig. 4.12: Higher magnification (1600X) micrograph for an water quenched sample.

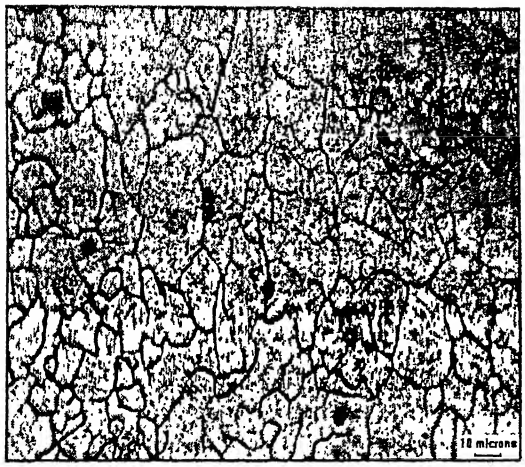

(a)

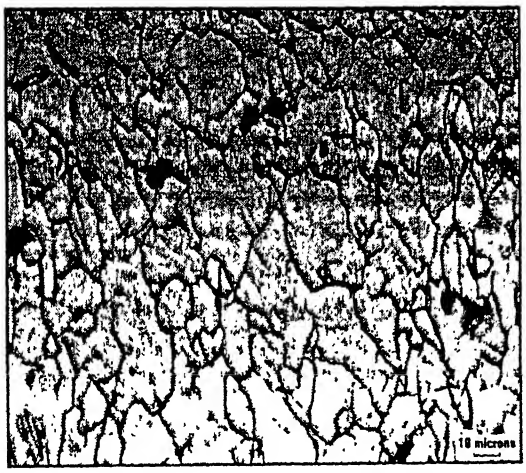

(b)

(c)

Fig. 4.13: Micrograph of water quenched samples showing grain boundaries (a) WQ1, (b) WQ2 & (c) WQ3. Magnification: 200X.

was measured. The yield strength of air cooled, two-step cooled and water quenched sample is shown in Tables 4.3and4.4. The yield strength is maximum for air cooling and two-step cooling at rolling finish temperature, 750-800°C.In water quenched samples the yield strength is maximum at rolling finish temperature, 850 – 900°C. The minimum for all cooling sequences are at rolling finish temperature, 800 – 850°C(refer Table 4.3 and 4.4).

Figs.4.14, 4.15and 4.16 shows that the water quenched samples have the highest yield strength. The difference in yield strength is the largest between air-cooled samples and water quenched samples.

Ultimate tensile strength:

Ultimate tensile strength of thermomechanically treated 38MnSiVS6 steel under different processing routes is shown in Tables 4.3 and 4.4. From the result it can be seen that as expected, the UTS of water quenched samples are substantially higher than other samples. In case of air-cooled samples the UTS of AC1 and AC3 are similar. However, for rolling finish temperature of 800-850°C (AC2 samples), the UTS is significantly lower. Similar trend can be observed for the TSC samples also.

Figs. 4.14, 4.15and 4.16, show the change in UTS due to difference in cooling rate. The difference in UTS of water quenched and TSC samples for rolling finish temperature 800-850°C is much larger than that of rolling finish temperature, 750-800°C and 850-900°C. The air-cooled samples have much lower UTS than TSC and WQ samples.

Toughness:

Toughness of the samples was measured as the area under stress-strain curve, which was estimated from equation 3.5. Tables 4.3 and 4.4 show the change in toughness due to the thermo mechanical treatment. The toughness of water-quenched samples are more than the TSC and AC samples, since it has much higher strength with little % elongation difference. Toughness of AC samples increases with the decrease in rolling finish temperature, as shown in Fig.4.17. On the other hand, TSC samples show a minimum toughness at rolling finish temperature 800 to 850°C.

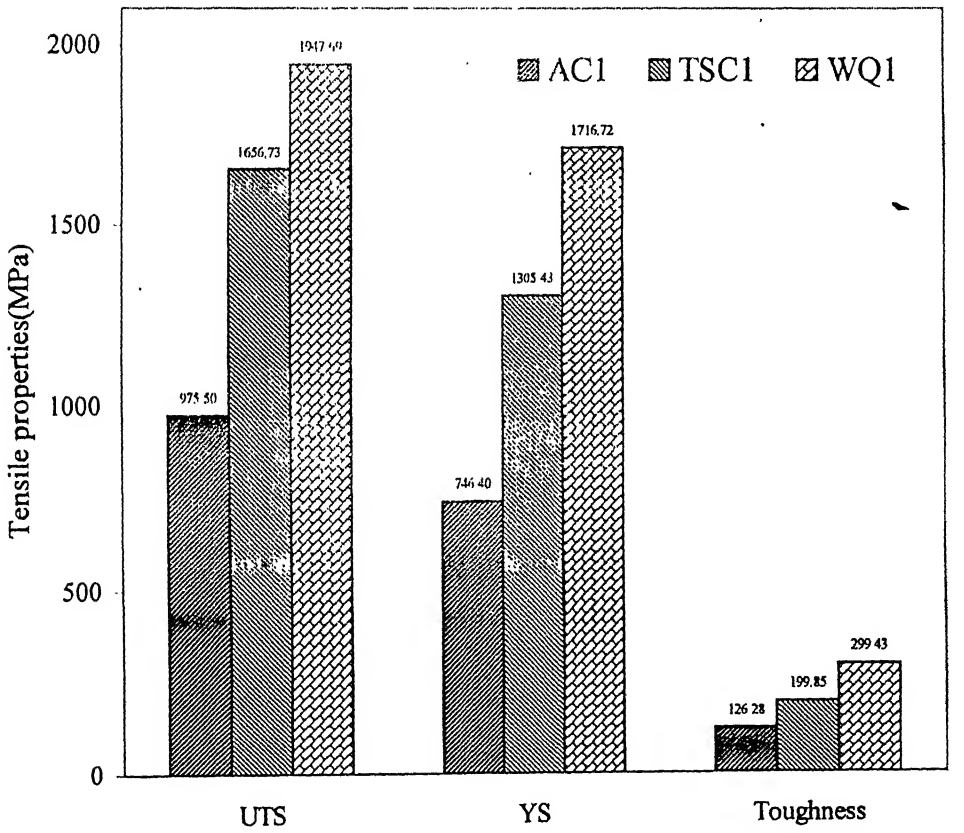

Fig.4.14: Variation of tensile properties with cooling sequence at rolling finish temperature, 850-900°C.

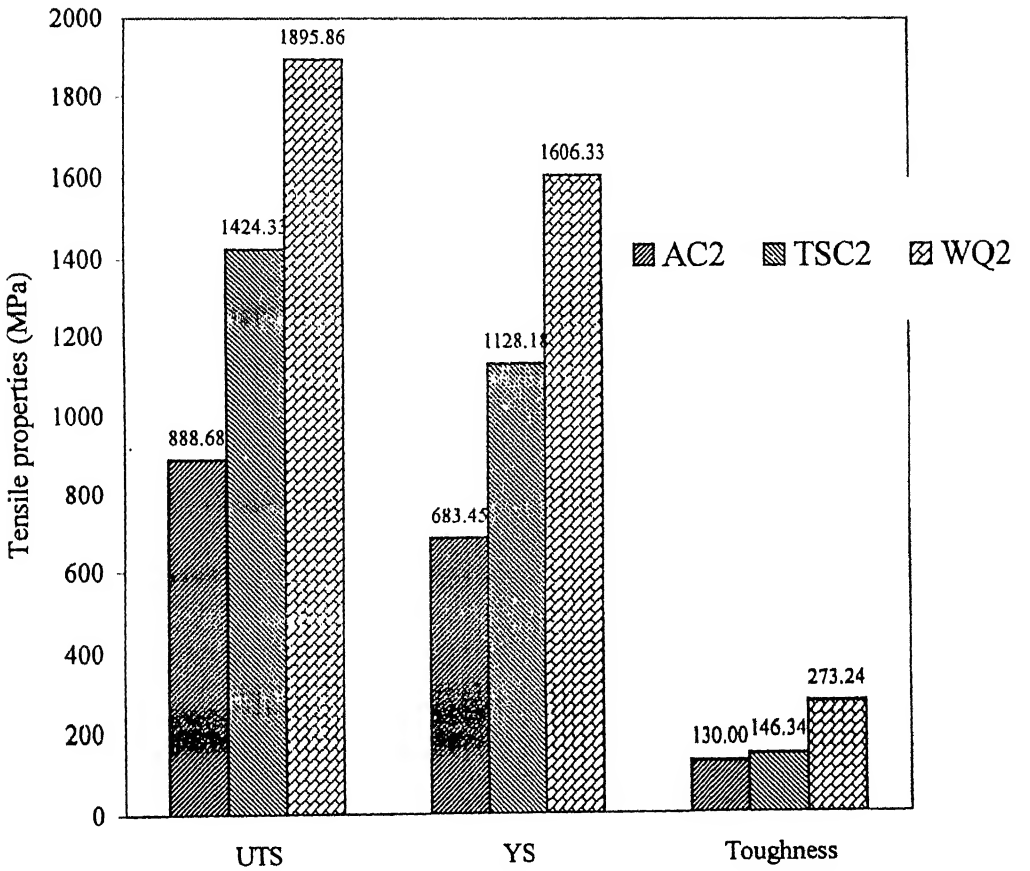

Fig.4.15: Variation of tensile properties with cooling sequence at rolling finish temperature, 800-850°C.

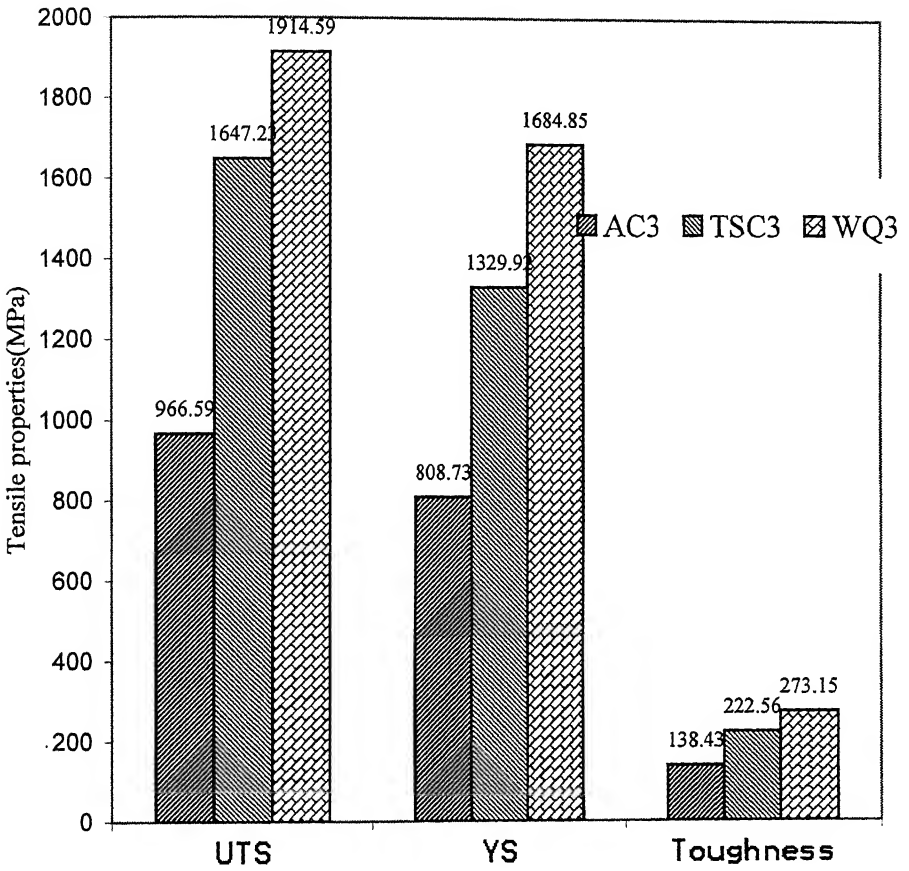

Fig.4.16: Variation of tensile properties with cooling sequence at rolling finish temperature, 750-800°C.

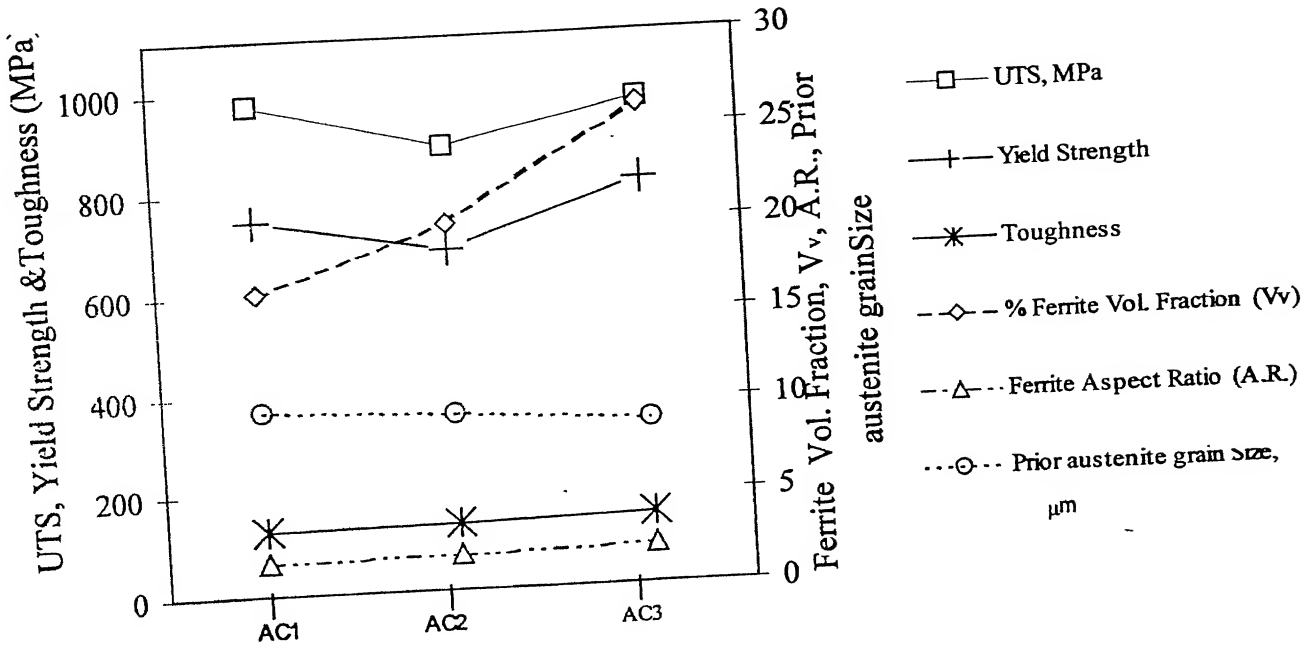

Fig: 4.17: Effect of rolling finish temperature on air cooled sample.

As shown in Figs.4.14, 4.15and 4.16 the toughness varies with cooling rate, water-quenched samples exhibit high toughness in contrast to air-cooled samples, which exhibit low toughness.

4.5 Processing structure-property correlations

4.5.1 Microstructural evolution during thermomechanical treatment

From the chemical composition of 38MnSiVS6 steel (shown in Table 3.1), it can be seen that it is medium –carbon microalloyed steel. Microstructural parameters of interest for manipulating its tensile properties (yield strength, ultimate tensile strength and toughness) of such steels are expected to be:

- Grain size of prior austenite grains,
- The volume fraction of carbide(s)/carbonitride(s) of the microalloying element(s), their size and size distribution,
- The amount of ferrite, its morphology, its size and the size distribution,
- Volume of bainite and/ or martensite as matrix in the microstructure.

Results shown in previous sections clearly show that most of the above microstructural parameters were influenced by the thermomechanical treatment schedules followed in the present investigation. Physical metallurgical considerations indicating that the thermomechanical treatment will influence the above microstructural features are discussed below.

The dissolution of carbides/ carbonitrides in the matrix of microalloyed steels is known to play an important role in the microstructural evolution of these steels during their thermomechanical treatments [41]. First, if the precipitates are not completely dissolved prior to rolling, the mechanical deformation occurs essentially of the austenite grains that are dispersed with carbide(s)/carbonitride(s). In such a case the carbon % of the austenite remains somewhat lower and hence the recrystallization temperature of steel is expected to be higher. The dissolution behavior of vanadium carbide has been studied using

thermodynamic considerations by several authors [14]. Precipitation and dissolution characteristics of vanadium and niobium carbides in austenite are shown in Fig.4.18

The rolling finish temperature has considerable effect on the microstructure and tensile properties of microalloyed steels. The structural changes in steels during rolling in three regions are schematically illustrated in Fig.4.19 and described below:

1 Deformation in recrystallization region- In this region, coarse austenite grains '**a**' are refined by repeated deformation and recrystallization, which produce the recrystallized grains '**b**'. During cooling these grains would transform into relatively coarse ferrite.

2 Deformation in non-recrystallization region: In this region deformation bands are formed in elongated, unrecrystallized austenite '**c**'. During cooling ferrite would nucleate on the deformation bands as well as γ grain boundaries, giving fine α grains '**c**'.

3 Deformation in the γ-α region: In this region, the deformation bands continue to be formed and also the deformed ferrite produces a substructure '**d**'. after deformation, during cooling, unrecrystallized austenite transforms into equiaxed α grains, while the deformed ferrite changes into the sub grains '**d**'.

In continuous hot rolling, the rolling finish temperature controls the extent of ferrite nucleation. At lower rolling finish temperature, the alpha grain nucleation occurs both in the grain interior and grain boundaries as would be for AC3 schedule. Since the grain boundaries as well as subgrain boundaries are the sites of ferrite nucleation, the AC3 sample (in comparison to AC1 and AC2) shows smaller pearlite colony size and larger ferrite volume fraction (see Fig. 4.17). The pearlite colony size measured (see Table 4.2) for air-cooled samples decrease with the decrease in rolling finish temperature, minimum for AC3 (13.03μm).

The formation of pearlite/martensite is highly dependent on cooling rate and composition of steel, while the hardenability of steel also depends upon the size of sample. Smaller the sample thickness larger will be the extent of martensite formation and higher will be the hardenability. As in the case of water quenched (WQ) samples, the cooling rate is fast and sample thickness is less resulted into martensitic structure.

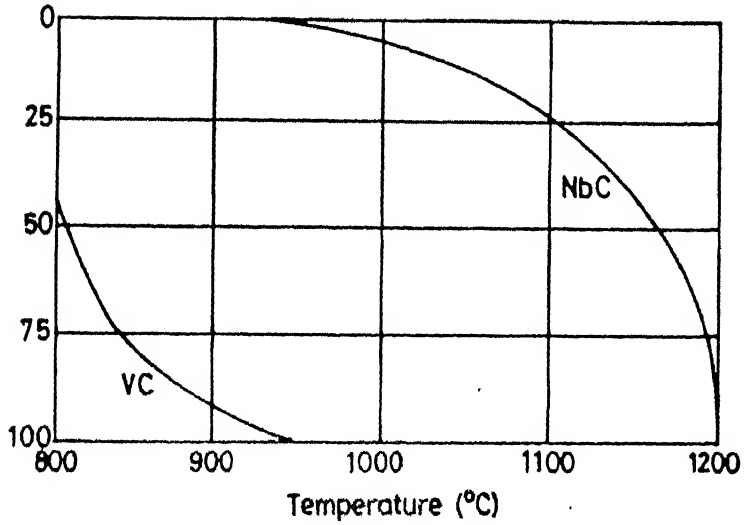

Fig. 4.18: Precipitation and dissolution characteristics of vanadium and niobium in austenite

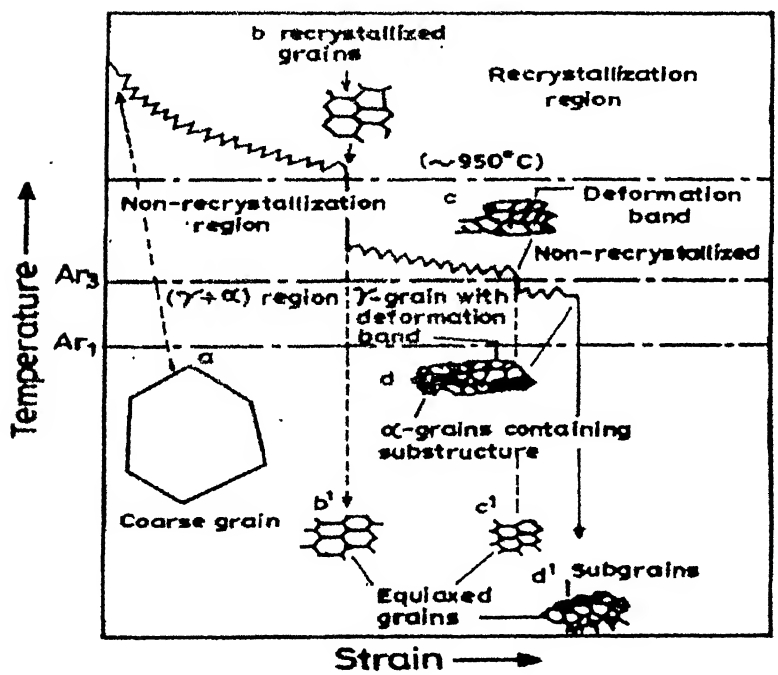

Fig. 4.19: Structural changes during rolling

In AC1 the higher UTS and yield strength but lower toughness is due to the presence of lower volume fraction of polymorphic ferrite (softer phase) and higher amount of pearlite (harder phase) than that of AC2 samples. In AC3 the presence of idiomorphic ferrite in the matrix of pearlite and with the increase in total volume fraction of ferrite the UTS, yield strength and toughness increases as shown in the Fig.4.17. The minimal increase in aspect ratio can be seen because of increasing trend of ferrite volume fraction with the decrease in rolling finish temperature.

The two-step cooled sample reveals mixture of polygonal ferrite and martensite with a small amount of idiomorphic ferrite. The trends found in TSC samples as shown in Fig. 4.21 are different from the AC samples, Fig. 4.17 due to the change in matrix morphology because ferrite growth is time and temperature dependent. The volume fraction of ferrite increases and then decreases with the rolling finish temperature. At lower rolling finish temperature, 750-800°C the time required for ferrite growth is not sufficient, because the quenching starts at the constant temperature, 650-700°C (see Fig. 3.3). In comparison to iron-carbon diagram it can be seen that critical temperatures are lowered due to deformation. Tensile properties (UTS, yield strength and toughness) decrease and then increase because the volume fraction of ferrite (softer phase) increases and then decreases (see Fig. 4.21).

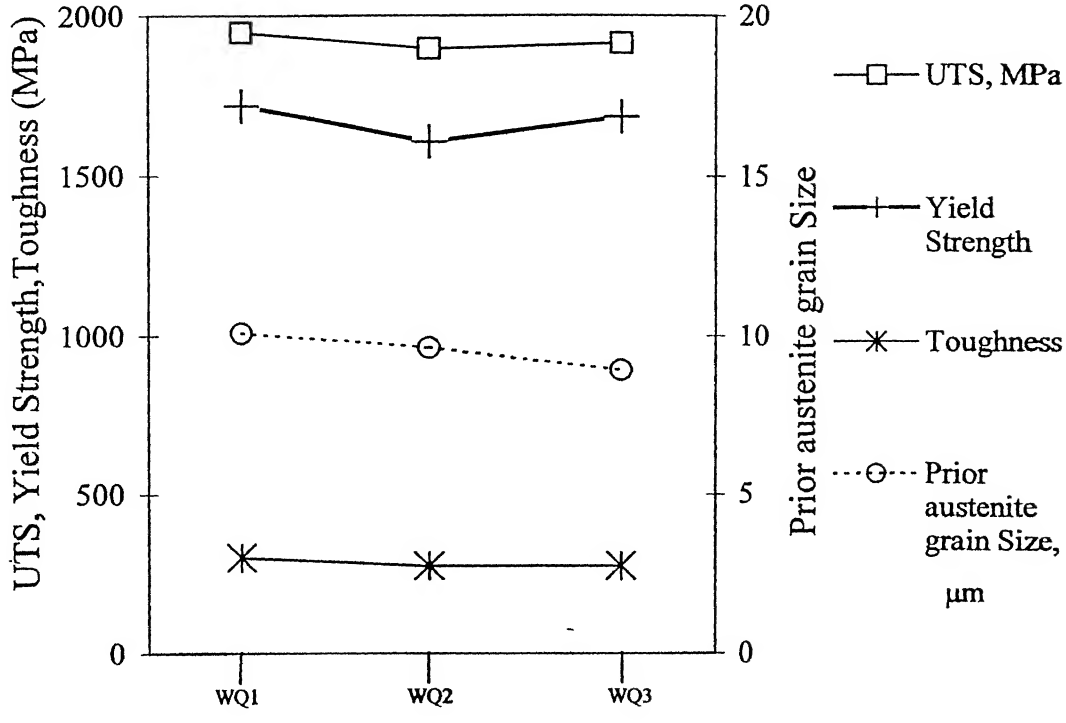

Fig. 4.20: Effect of rolling finish temperature on water quenched samples

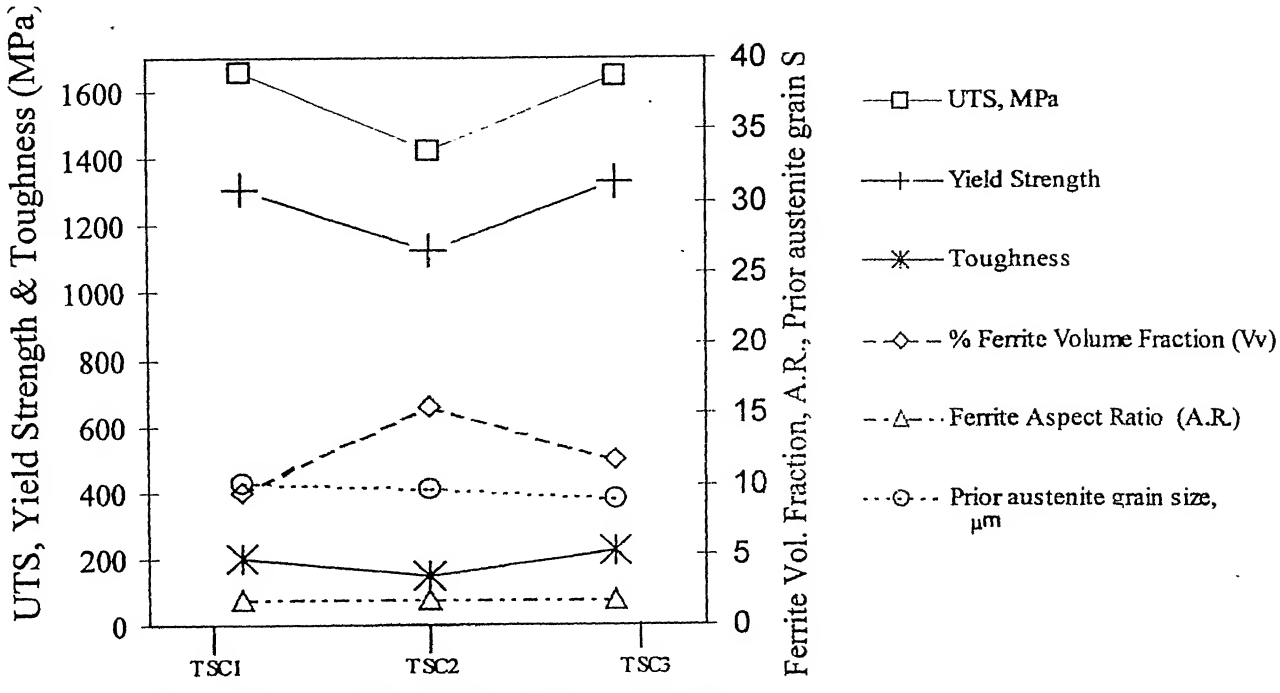

Fig.4.21: Effect of rolling finish temperature on two step cooled samples.

CHAPTER 5

CONCLUSIONS

Some major conclusions that have been resulted from the present investigations are

1 Thermomechanical treatments of 38MnSiVS6 steel play an important role in altering microstructural state and hence its mechanical properties.

2 Deformation start temperature has effect on amount of ferrite formation and its morphology, The complete dissolution of VC/V(CN) precipitates with maximum dynamic recrystallization at 1200°C , resulting in minimum volume fraction of ferrite as compared to lower deformation temperature. So, deformation start temperature of 1200°C is chosen for subsequent thermo-mechanical treatments.

3 Rolling finish temperature has good effect on mechanical properties of 38MnSiVS6.The rolling finish temperature 800- 850°C should be avoided to have good UTS, yield strength & toughness for both AC & TSC samples.

4 The rolling finish temperatures have no much effect on microstructure and tensile properties of water quenched samples.

5 The decrease in prior austenite grain size with rolling finish temperature for water-quenched samples have no effect on tensile properties.

6 The cooling rate dictates the matrix phase, the presence of martensite lead to have good measured tensile properties.

7 The ferrite morphology has effect on tensile properties with change in rolling finish temperatures for air-cooled and two-step cooled samples.

8 The prior austenite grain size at rolling finish temperature measured is very helpful in studying the trends of ferrite nucleation.

9 The presence of idiomorphic and polymorphic ferrite mixture in air-cooled sample at rolling finishes temperature 750-800°C lead to have good tensile properties.

SUGGESTIONS FOR FUTURE WORK

1. The effect of interlamellar spacing of pearlite on tensile properties for air-cooled samples can be studied.
2. Scanning electron microscope and transmission electron microscope should be used for the detailed study.
3. The influence of plate thickness on microstructure and mechanical properties with the same thermo-mechanical treatment may explore some interesting results.

REFERENCES

1. D.J. Naylor, in: *Proc. Int. Conference Microalloying in Steels*, Eds. J.M. Rodrigue-Ibabe, I. Gutieerez and B. lopez, Trans Tech Publications, Switzerland, (1998), 83.
2. Gonzalez-Baqet, R. Kasper and J. Richter, *Steel Research* 68 (1997), 61.
3. R. Kasper, I. Gonzalez-Baquet, N. Schreiber, J. Richter, G. NuBbaum and A. Kothe *Steel Research* 68 (1997), 27.
4. Gonzalez-Baquet, R. Kasper, J. Richter, G. NaBbaum and A. Kothe, *Steel Research* 68 (1997), 534.
5. R. Kasper, I. Gonzalez-Baquet, J. Richter, G. Nabaum and A. Kothe, *steel Research* 68 (1997), 266.
6. *Metals Handbook* vol8, Metals Park, ASM, 34.
7. M.F. Ashby, *Phil. Mag.* 14 (1966), 1157.
8. L.M. Brown and M.M. Stobbs, *Phil. Mag.* 23 (1971), 1185.
9. N.K. Ballinger and T. Gladman, *Met. Science* 15 (1979), 95.
10. C.A.N. Lanzillotto and F.B. Pickering, *Met. Science* 16 (1982), 371.
11. L.F. Porter, in: *Encyclopedia of Materials Science and Engineering* 3,Permagon Press and MIT Press, (1986), 2157.
12. L. Meyer, F. Heistterkamp and W. Mueschenborn, in: *Microalloying 75*, Ed. M. Korchensky, New York: Union Carbide Corporation (1977), 153.
13. T. Gladman and F.B. Pickering, *J. Iron Steel Inst. London* 205 (1967), 653.
14. P.H. Wrigth, in: *Metals Handbook 1*, Eds. J.R Davies et. al., Metals Park, OH: ASM (1990), 358.
15. St. Zajac et. al., in: *Microalloying 95*, Iron and Steel Society (1995), 140.
16. R. Lagneborg et. al., *Scand. J. of Metallurgy*. 28 (1999), 173.
17. P.J. Lubensky et. al., in: *Microalloying 95*, Iron and Steel Society (1995), 193.
18. M. Korchynsky and St. Zajae, in: *Proc. Thermomechanical Processing in Theory, Modelling and Practice*, ASM International, Stockholm (1996), 76.

19. R.K. Amin and F.B. Pikering, in: *Thermo-mechanical processing of microalloyed Austenite*, Eds. A.J. De Ardo, G.A. Ratz, P.J. Wray and P.A.Warrendale, AIME (1982), 1.
20. T. Tanaka, N. Tabata, T. Hatomura and C. Shinga, in: *Microalloying 75*, Ed. M. Korchensky, Union Carbide Corporation, New York (1977), 88.
21. T. Tanaka, *Int. Met. Reviews* 4 (1981), 185.
22. W. Roberts, A. Sandberg, T. Siwecki and T. Werlefors, in: *HSLA Steels Tech.*. Ed. M. Korchynsky, Metals Park (1984), 67.
23. Y.Z. Zheng, G. Fitzsimons and A.J. De Ardo, in: *HSLA Steels Technology and Applications*, Ed. M. Korchynsky, Metals Park (1984), 85.
24. R.M. Fix, Y.Z. Zheng and A.J. De Ardo, in: *HSLA Steels-Metallurgy and applications*, Eds. J.M. Gray et. al., Metals Park, OH:ASM (1986), 219.
25. M. Korchynsky and H. stuart, in: *Low Alloy High Strength Steels*, Number Metallurgy (1990), 17.
26. S. Zajac, T. Siwecki, B. Hutchinson and M. Attlegard, in: *Microalloyed Vanadium Steels*, Eds. M. Korchynsky et. al., Association of polish Metallurgical Engineers and Strategic Minerals Corp. (1990), 149
27. M. Korchynsky, in: *Microalloyed Vanadium Steels*, Eds. M. Korchynsky et. al., Association of Polish Metallurgy Engineers and Strategic Mineral Corp. (1990) 5.
28. J.S. Kirkaldy, *Metall. Trans.*, 4 (1973), 273.
29. R.C Sharma and G. Purdy, *Metall. Trans.*, 5 (1974), 939.
30. H.K.D.H. Bhadeshia, Met. Sci., 16 (1982), 159.
31. M. Unemoto, A. Hiramatsu, A. Moriya, T. Watanabe, S. Nanaba, N. Nakajima, G. Anan and Y. Higo, *ISIJ Int.*, 32 (1992), 306.
32. R.C Reed and H.K.D.H Bhadesia, *Mater Sci. Technol.*, 8 (1992), 421.
33. I. Madariaga and I. Gutierrez, C. Garcia de Andres, C. Capdevila, *Scripta Mater.*, 41 (1999), 229.
34. H.K.D.H Bhadesia, *Mater. Sci. Tech.*, 1 (1985), 497.
35. A. Blarasin and P. Faretti, *Int. J. Fatigue*, 11(1989), 13.
36. L. Yang and A. Fatemi, *J. Testing Evaluation* 23 (1995), 80.
37. Y.H. Kim and M.E. Fine, *Metall. Trans.*, 13A (1982), 80.

38. G.F. Vander Voort, in: *Metallography Principles and Practice*, ASM Int., (1999), 637.
39. G.E Dieter, in: *Mechanical Metallurgy*, McGraw Hill, (1988), 283.
40. T. Tanaka, in: *Int. Met. Rev. American Society for Metals*, Metals Park (1981), 185.